Electronic Supplementary Material (ESI) for Materials Advances.

SUPPORTING INFORMATION

A Review of Metal, Metal-Oxide, and Semiconductor Nanoparticle Syntheses Using In Situ Synchrotron XAFS and SAXS en Route to Particle Formation Mechanisms

Christopher B. Whitehead and Richard G. Finke*

Department of Chemistry, Colorado State University, Fort Collins, CO 80523, USA

Contents of this Supporting Information Section

Following additional information for case studies, there are four literature summary tables. These tables, S1–S4, contain the 74 papers that were analyzed for this review. The following is provided for each paper: (i) a presentation of the system and techniques used to study it; (ii) a synopsis of the reported results; and (iii) a critical analysis of the conclusions. A complete list of abbreviations may be useful and can be found at the end of the supplementary documents. Common abbreviations for some of the models and mechanisms discussed in the tables are: AE = Avrami-Erofe'ev[1,2,3]; CNT = Classical Nucleation Theory[4,5,6]; FW = Finke-Watzky (2-Step Mechanism)[7]; and LSW = Liftshitz-Slyozov-Wagner[8,9]. Additionally, disproof-based[10,11] critical analysis is used when assessing the conclusions of the 74 papers. Finally, every attempt was made to remain unbiased and present only the details of the paper and provide a critical analysis of those results, the same approach at least striven for in our three recent reviews and critical analysis [12,13,14] of the 1950 LaMer model[15].

Case Study #2: Additional Figures and Information

Below as Figures S1–S3, the accompanying MALDI-TOF mass spectra of the EXAFS experiments (Figure 5, main text) on the $RhCl_3$–TTAB–PVP–EG system are given.[16]

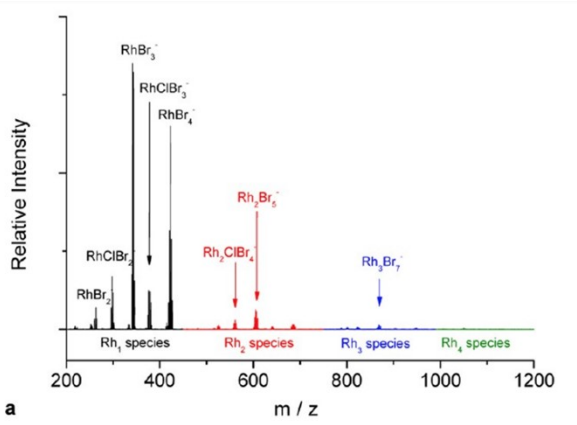

Figure S1. Negative ion MALDI-TOF mass spectra of the same $RhCl_3$–TTAB–PVP–EG system as shown in Figure 5 (main text) at 3 min after reduction. Figure reproduced in part with permission from ref 16. Copyright 2012 American Chemical Society.

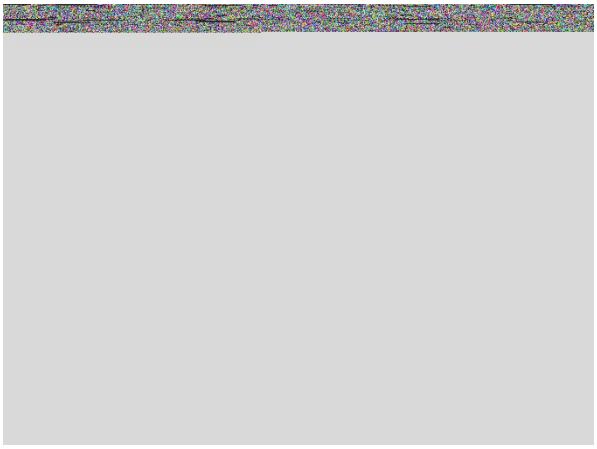

Figure S2. Negative ion MALDI-TOF mass spectra of the same $RhCl_3$–TTAB–PVP–EG system as shown in Figure 5 (main text) at 15 min after reduction. Figure reproduced in part with permission from ref 16. Copyright 2012 American Chemical Society.

Figure S3. Negative ion MALDI-TOF mass spectra of the same $RhCl_3$–TTAB–PVP–EG system as shown in Figure 5 (main text) at 20 min after reduction. Figure reproduced in part with permission from ref 16. Copyright 2012 American Chemical Society.

Differential Equations for the Karim 4-Step Mechanism

Set of differential equations (Eqs S1-S5) that accompany the entry in Table 1 of the main text on the Karim 4-step, mechanism accounting for ligand, L, effects. These differential equations result from the mechanism given in both Table 1 and in Scheme 1 in the main text.

$$\frac{\mathrm{d}[A]}{\mathrm{d}t} = -k_{1-nuc}[A] - k_{2-growth}[A][B] - k_{3-f}[A][L] + \frac{k_{3-f}}{K_{5-eq}}[AL] \qquad \text{(Eq S1)}$$

(Eq S2)

(Eq S3)

(Eq S4)

(Eq S5)

Table S1. Summary of Reviews on Synchrotron XAFS and/or SAXS.

Entry	Title	Topic of the Review	Valuable Insights from the Review for the Scientific Community	Specific Points We Wish to Highlight from the Review	Ref.
1	Characterization of nanoparticles by scattering techniques	The review is focused on scattering techniques for characterization of nanoparticles. "The emphasis is on specific applications to determine the size, shape, and structure of particles, especially nanoparticles, by using the scattering techniques."[17]	The review has excellent background sections covering the theoretical foundation of SLS versus DLS and SAXS versus SANS. Next, the authors have provided guidance to researchers using angular dependence techniques to determine nanoparticle (i) size, (ii) shape, and (iii) internal structure. Then, the authors provide guidance to researchers re: determining the nanoparticle (i) hydrodynamic radius, (ii) particle size distribution, and then for anisotropic particles (iii) rotational diffusion coefficient.	This review article has an excellent section of derivations for "basic scattering functions". Next, the review covers the specific differences between time-averaged scattering techniques and intensity–intensity time correlation techniques. Finally, the review concisely concludes that "using a combination of different scattering techniques can provide much richer and complementary information on the specific systems."[17]	17
2	Use of SANS and SAXS in study of nanoparticles	The review is focused on the use of SANS, SAXS, or tandem SANS/SAXS to study nanoparticles. The review covers background knowledge of SANS and SAXS, the concept of Contrast Factor, and a case study of researching micelles using SANS/SAXS.	The two different techniques, SANS and SAXS, both have great value when researching micellular species. "For example SAXS experiments on gold nanoparticles will give information about the size of the core"[18] Whereas, "neutrons are largely scattered from hydrogenous material of the capping which constitutes the outer shell of Au nanoparticles."[18] Conversely, for micelles composed of hydrogenous materials, "neutrons see the core of the micelle and X-rays give information about the shell of counterions around the micelle."[18]	Of particular note, the two techniques are highly sensitive. The authors cover a case study where micelles were prepared from 100 mM solutions of sodium dodecyl suphate (SDS) and cetryltrimethylammonium chloride/bromide (CTAC / CTAB). The micelles prepared from SDS/CTAC exhibited similar SANS and SAXS patterns. However, the micelles prepared from SDS/CTAB were dramatically different. The techniques (SANS and SAXS) are extremely "sensitive to even small changes in the thickness of the shell" of the micelle.[18]	18
3	Combining *in situ* characterization methods in one set-up: looking with more eyes into the intricate chemistry of the synthesis and working of	The review by Dr. Ursula Bentrup is focused on the tandem use of several *in situ* characterization techniques to monitor the formation and activity of heterogeneous catalysts. She provides a "*tutorial review*…of	Dr. Bentrup presents numerous excellent points about the use of tandem *in situ* techniques to monitor particle formation and reaction progress. First, is that each method used "has its own potentials, limitations, and special requirements."[19] Hence, it is necessary to understand what the technique's capability is and only apply it to that.	In particular, we wish to highlight Table 1 (Overview of available *in situ* techniques together with the specific information to be obtained) and Table 2 (Overview of existing combinations of *in situ* techniques and selected studied reactions). These are a *must read* for anyone preparing to use direct *in situ*	19

	heterogeneous catalysts	currently available set-ups equipped with multiple techniques for *in situ* catalyst characterization, catalyst preparation, and reaction monitoring."[19]	Second, from "looking at the specific information available from…different techniques it is evident that only a combination or coupling of different methods enables a comprehensive picture of the working catalysts in the particular reaction" of interest.[19] And third, "it has to be realised that no universal multitechnique set-up exists solving all problems because each applied *in situ* method has specific technical requirements, advantages and disadvantages, and provides definite information."[19]	techniques to monitor their reaction. Furthermore, it is imperative that one remains vigilant of the limits of a given technique and not interpret their results beyond what the data allows.	
4	In Situ Synchrotron X-Ray Techniques for Real-Time Probing of Colloidal Nanoparticle Synthesis	The review by Y. Sun and Y. Ren provides foundational information on a series of X-ray techniques (XAFS, SAXS, XRD, PDF, TXM, WAXS, and X-ray Raman) for the in-situ study of solution nanoparticle formation. The authors include a series of case studies and *personal* perspectives on the use of the different X-ray techniques.	First, in section 3, TXM is understood to best work with particles between 50-2000 nanometers and "is capable of controlling image contrast of different elements by tuning X-ray energy".[20] In section 4, different variations of XAFS are analyzed. Of note, when dealing with *fast* reaction kinetics, DXAFS is most advisable, but one will lose some energy resolution due to the speed of the measurements. A final, important section to highlight is section 5.3 "In Situ Total Scattering Pair Distribution Function (PDF)"[20]. If PDF is appropriate for one's system, the PDFs "control structural information beyond the first few coordination shells that represents the major information of the XAFS data." Further, "the bond length between atoms derived from the PDFs are the absolute values while the distances extracted from the XAFS measurements are always subject to an offset or derived from a structural model."[20]	We wish to point the reader to Table 1, Figure 6, and Figure 12 within ref 20. Table 1 is a "summary of the in situ synchrotron X-ray techniques for studying colloidal nanoparticle synthesis".[20] Figure 6 shows SAXS scattering patterns for "particles with ideal geometries."[20] Figure 12 presents a "summary of possible processes involved in the growth of shaped nanoparticles made of face-centered cubic metals in liquid solutions as well as the potential capabilities of different in situ techniques for probing different process."[20] Finally, the reader should be mindful when going over ref 20 because it is an excellent source to obtain a foundational understanding for a series of different X-ray techniques, it is not recommended for understanding mechanistic investigations.	20
5	Small Angle X-ray Scattering for Nanoparticle Research	The review by Lee and co-workers is one of the most extensive in the literature today. It covers the majority of topics with the primary		We recommend this review to anyone that is interested in SAXS and would like to learn from this important review.	21

	sections being on the following: (1) Introduction, (2) Data Measurement and Processing, (3) Particle Scattering, (4) Correlation Function Approach, (5) Combination of Scattering with Model Simulations, (6) GISAXS, (7) Applications, and (8) Conclusions and Outlook.	

Table S2. Summary of Papers Using SAXS to Collect Kinetics Data.

Entry	Title	System & Techniques Used to Monitor the Kinetics	Results and Proposed Chemical Mechanism	Conclusions, Insights, and Critical Analysis	Ref.
1	Small-angle x-ray scattering analysis of polymer-protected platinum, rhodium, and platinum/rhodium colloidal dispersions	The authors studied the formation of three types of colloidal dispersions: platinum, rhodium, and 1:1 platinum/rhodium; all as polymer-protected dispersions. Aqueous metal salt solutions of hexachloroplatinic(IV) acid and rhodium(III) chloride were prepared. Next, ethanol solutions of PVP were prepared. The two solutions were mixed at 100 ºC, with stirring, and under N_2 gas. Measurements were collected using SAXS, and final particle size and size-distributions were determined using TEM.	Based on their results, the authors hypothesized the formation of their particles follows "three fundamental process… (I) formation of polymer–metal ion complexes, (II) reduction of metal ion complexes and formation of metal atoms, and (III) association of the metal atoms to form the elementary metal clusters."[29] The elementary metal clusters for the three systems are composed of magic number clusters, "i.e., Pt_{55}, Rh_{13}, and $[(Pt/Rh)_{55}]$."[29] "In addition to the processes described above, there is a process leading to formation of the higher-order organization of the superstructure; (IV) agglomeration of the elementary metal clusters into the superstructures and their higher-order organizations."[29] Finally, "[t]he hierarchy observed in the order of decreasing size is as follows: higher-order organization of superstructures>superstructure of fundamental metal clusters>fundamental metal cluster>elementary metal cluster composed of magic number of atoms."[29]	The results presented by the authors are fascinating. They demonstrate the application and benefit of using SAXS on a nanoparticle, colloidal-metal system. Of note, the authors have not attempted to *claim* a mechanism, but rather have presented a hypothesized reaction pathway with pseudo-elementary steps. The mass-balance and kinetics have not been determined, nor have alternative, competing hypotheses been disproven, but, again, the authors have not made claims beyond what the data allow. Intriguingly, with 22 years of hindsight one can now say that the authors have presented fascinating evidence for polymer–metal ion complexation indicative of "prenucleation clusters".[22,23,24,25,26,27,28] This growing concept necessitates additional study while including this paper as recommended background literature.	29
2	Small-Angle X-ray Scattering Study of Platinum-Containing Hydrogel/Surfactant Complexes	Platinum nanoparticles were prepared from a series of different platinum-containing starting materials, reducing agents, and stabilizers. The platinum compounds were $PtCl_4$, Na_2PtCl_6, $(NH_4)_2PtCl_4$, and H_2PtCl_6. The two reducing agents were $NaBH_4$ and $N_2H_4{\bullet}H_2O$. The cation gel was	The authors found that $N_2H_4{\bullet}H_2O$ was a slower reducing agent and "yielded much larger nanoparticles than the fast $NaBH_4$."[30] The $PtCl_4^{2-}$ starting material yielded smaller particles with narrower size distributions than $PtCl_6^{2-}$, all in the cationic gel/anionic surfactant. Meanwhile, in the anionic gel/cationic surfactant, much larger particles were observed "where the particle growth is	The authors of this study have presented an excellent *proof of concept*, where the use of SAXS and ASAXS are shown to provide excellent, direct, quantitative experimental results and details. These authors have investigated the effects of different variables on the final nanoparticles size distribution. Most importantly, the authors have not attempted to claim results beyond what the data have shown. They suggest reaction	30

		poly(diallyldimethylammonium chloride) (PDADMACl) with either sodium dodecyl sulfate (SDS) or sodium dodecylbenzene sulfonate (SDBS), both anionic surfactants. The anionic gel / cationic surfactant combination was poly(methacrylic acid) and cetylpyridinium chloride (PMA/CPC). Reactions were run in water under argon. Characterization was done with SAXS and elemental analysis. SAXS measurements were collected using the Pt L_3-edge.	not controlled by the internal gel structure."[30] The authors conclude "that the highly ordered zones in the hydrogels concentrate around the growing nanoparticles."[30] Finally, the authors claim "the obtained results illustrate the potential of the SAXS and ASAXS methods allowing systematic selection of metal compounds and reducing agents for the preparation of metal nanoparticles with desired size distributions as well as quantitative characterization of the ordering phenomena in the gel/surfactant complexes."[30]	pathways, that can now be investigated for the additional evidence (fitting of kinetics data and complete speciation/known stoichiometry) needed before a reliable mechanism can be claimed.	
3	Synthesis of Ultra-small ZnS Nanoparticles by Solid-Solid Reaction in the Confined Space of AOT Reversed Micelles	Small ZnS nanoparticles were prepared in reverse micelle synthesis. AOT (sodium bis(2-ethylhexyl)sulfosuccinate) and *n*-heptane were used to prepare the reverse micelles. The ZnS nanoparticles were made from the solid-solid mix of zinc sulfate and sodium sulfide. The reaction occurred at 22 ºC and studied by UV spectroscopy and SAXS.	The formation reaction was observed to occur on a fast time scale. The resulting nanoparticles were seen to be small, ~2 nm in diameter. In depth investigation revealed that "the coupled analysis of SAXS and UV spectra suggested that the energy gap does not uniquely depend on the nanoparticle size, but one more factor such as atomic arrangement could be involved."[31]	This study is not on the mechanism of the particle formation, but rather on demonstrating a new approach to preparing two-component nanoparticles using a solid-solid synthetic approach. Of note, the authors are careful to not overstate what their data means. In fact, in several instances, they recognize the limitations of their instrumentation and the need for addition investigations using WAXS, EXAFS, XPS, and so on. This is a fundamental, proof-of-concept study, one that does not strive to provide kinetics or mechanistic insights.	31
4	From Pt molecules to nanoparticles: *in-situ* (anomalous) small-angle X-ray scattering studies	Platinum colloids were prepared from $Pt(acac)_2$ in toluene under argon at 333 K. Over 4 hours, $Al(CH_3)_3$, also in toluene, was slowly added. The reaction ran for ~24 hours until the solution changed from yellow to black and gas evolution had stopped. Characterization was done ex situ by quenching the aliquot to	The authors present ASAXS results of their $Pt_{\sim 53}$ nanoparticle system stabilized by what they call an organic shell. ASAXS data was collected on quenched reactions between 0.8 and 63 hours at room temperature. The authors found that "with increasing reaction time, the scattering intensity increases by half an order of magnitude, whereas the overall shape of the scattering curves remains	Of note, the authors have used the "anomalous scattering from the metal atoms [to separate] the superimposed small angle scattering contributions from particles and the organic molecules in the solvent."[32] However, the analysis of the results are plagued by attempted *proof*-based and confirmation-bias laden experimentation, in which the experiments are designed to try to *prove* the author's conclusions—rather than the needed	32

		195 K with liquid nitrogen. Measurements were taken using NMR (^{1}H, ^{13}C, and coupled to ^{195}Pt), XANES, ASAXS, TEM, and DFT. This report was focused on the ASAXS studies.	essentially unchanged."[32] Then, they authors attempted to fit their kinetics data with an exponential power function. Finally, they claim "the nucleation of Pt nanoparticles with a rather narrow size distribution."[32]	disproof of multiple alternative hypotheses. Further, the claim of a "narrow size distribution"[32] is not substantiated with any direct TEM images, size distributions, or even error associated with the average particle size. Finally, the kinetics data were 'fit' using a semi-empirical exponential function, that in essence is just the Avrami-Erofe've equation. Yet, there was no explanation for the use of the exponential function, nor did its use provide any valuable information on the mechanism or potential reaction pathways for the formation of $Pt_{\sim 53}$. Hence, considerable caution is recommended when reading this paper or using its contents or conclusions.	
5	Physicochemical investigation of surfactant-coated gold nanoparticles synthesized in the confined space of dry reversed micelles	Gold nanoparticles were synthesized inside of two dry reversed micelles, AOT (sodium bis(2-ethylhexyl)sulfosuccinate) and lecithin. The gold precursor used was tetrachloroauric acid and the reductant was hydrazine. The systems were characterized by UV-vis, FT-IR, WAXS, and SAXS.	FT-IR analysis of the dry reversed micelles with gold precursor revealed no distinguishable presence of water. UV-vis was used to show the loss of the d-d transition at 320 nm, indicative of $AuCl_4^-$, and the appearance of the signal at 528 nm, indicative of small-sized Au(0) nanoparticles. WAXS analysis suggests, that by either method, nanoparticles were formed with a radius of 1.4 ± 0.2 nm. SAXS results produced a size equivalent within experimental error. Overall, the authors claim to have "shown that a simple treatment with ethanol is able to eliminate the excess of surfactant not directly bound to the nanoparticle surface" and that "nanoparticle size does not seem to be modified by this treatment."[33]	The authors have demonstrated the value of X-ray scattering techniques (SAXS and WAXS). Importantly, they have not attempted to draw conclusions beyond the data that they have collected. In addition, they state further investigations are required.	33
6	Synthesis of Ruthenium Nanoparticles Stabilized by Heavily Fluorinated	Ruthenium nanoparticles were prepared under H_2 from Ru(COD)(COT) in THF and stabilized by heavily fluorinated compounds, where COD = 1,5-	The $Ru(0)_n$ nanoparticles were found by TEM and SAXS to be 2.9 nm in size with a dispersity of ca. 20%. These particles were found to aggregate into larger 50-100 nm spherical clusters. Of note, they	This system is of particular interest for mechanistic study as it has several direct as well as indirect physical handles and also produces stable, reproducible particles. Two main things that are needed are (i) kinetics data	34

	Compounds	cyclooctadiene and COT = 1,3,5-cyclooctatriene. The resulting $Ru(0)_n$ nanoparticles were characterized by FT-IR, elemental analysis, HR-TEM, WAXS, SAXS, and SEM-FEG.	are not observed to coalescence into a giant particle. The authors hypothesis that "[t]he coalescence of the particles may be prevented by the presence of the fluorinated stabilizer acting as a coating protective barrier."[34]	for the formation of the $Ru(0)_n$ nanoparticles, and (ii) differential equations to describe the pseudo-elementary step reactions.	
7	Probing in situ the Nucleation and Growth of Gold Nanoparticles by Small-Angle X-ray Scattering	Gold nanoparticles were prepared by combining gold(III) chloride in toluene with tetrabutylammonium borohydride in the presence of either decylamine or decanoic acid. The cationic surfactant, didodecyldimethylammonium bromide, was used. The gold salt and the reducing agent (with ligands—either amine or acid) were combined using a stopped flow device. The reaction was monitored in real time using either UV-vis, SAXS, or WAXS.	The authors "observe that the final radius strongly depends on the chemical nature of the ligand (3.5 nm for the acid, 1.4 nm for the amine)."[38] The authors interpret the reaction kinetics data, collected using both UV-vis and SAXS, by applying CNT. Furthermore, they use "a generic differential equation"[38] to calculate the rate of growth of the particles. Finally, they conclude that "the final size of the particles is thus controlled by the very first instant of the reaction that these experiments are able to probe: the higher the nucleation rate, the smaller the final particle size. [Their] results thus unambiguously prove the pioneering hypothesis[35] of Frens."[38]	The authors have concluded, from their size versus time data, the chemical nature of the gold nanoparticle and ligand interactions. The authors have investigated the aspects of their data that support their hypothesis—whereas with mechanism, one needs to consider all reasonable alternative hypotheses.[10,11] Ligands, for example, are known to contribute *greatly* to controlling the *growth step*.[21] Additionally, the kinetics have been analyzed on the basis of CNT, which is unable to encapsulate the strong bonding in metal nanoparticle nucleation.[36,37] Therefore, reliable mechanistic understanding is not forthcoming from the kinetics analysis provided.	38
8	In Situ Small-Angle X-ray Scattering Observation of Pt Catalyst Particle Growth During Potential Cycling	The size of catalytically active Pt nanoparticles was monitored by SAXS during potential cycling. The system used was Pt on carbon (20 or 40 weight % platinum on XC-72 Vulcan carbon). The electrode was placed in 0.1 $HClO_4$ against a carbon counter electrode and Ag/AgCl reference electrode. Potentials were cycled from 0.4 to 1.4 V.	Over the 16 hours of testing, the particles are observed to grow continuously. The authors present a plot of the Pt nanoparticle size as a function of time over three potential cycles, where the particle growth appears to be "cycling with reversible and irreversible components."[39] The growth with potential cycling is observed to be small and "attribute[d] to oxide formation."[39]	The authors have presented a fascinating study of the effects of potential cycling on the growth of nanoscale electrocatalysts. They have proposed a preliminary "potential mechanism for potential cycling-induced particle growth."[39] Unfortunately, this proposed mechanism has not been tested by the authors in this communication. The kinetics data need to be fit using the full integrated form of the differential rate equation based on the balanced stoichiometry.	39
9	Characterization of metal nanoparticles prepared by photoreduction in	Au and Pt colloids were prepared from eterachloroauric(III) acid and hexachloroplatinic(IV) acid in	The UV-vis display that the Au colloids are formed rapidly without about 15 minutes, while the Pt colloid formation takes longer. The TEM of Pt and Au	The authors claim that "photoreduction formation mechanisms of metal particles in aqueous surfactant solution…were successfully investigated."[40] However, no	40

	aqueous solutions of various surfactants using UV-vis, EXAFS, and SAXS	water. The stabilizers DTAC (dodecyltrimethylammonium chloride) and PEG (polyethylene glycol lauryl ether) were used in varied concentrations. Colloidal dispersions were made by irradiated the solutions with a 500 W super-high-pressure mercury lamp. Primarily, the colloidal products were characterized by SAXS. Additional, ex situ measurements were collected using EXAFS, UV-vis, and TEM.	colloids in the presence of 151x DTAC concentration resulted in an average diameter of 4.1 nm. The TEM of Pt and Au colloids in the presence of 151x PEG concentration resulted in an average diameter of 3.3 and 3.4 nm, respectively. No error range was given with the TEM results. The TEM results are in agreement with the SAXS results. No mechanism for particle formation is given. None of the kinetics data are fit.	mechanisms were proposed, and no kinetics data were fit. Furthermore, the authors claim in their conclusions that "the SAXS analysis indicated that the structure of surfactant micelles could be fitted by the hard-sphere model with the interaction radius R_{HS} and the spherically shaped core-shell structure."[40] While the authors are proposing this hypothesis based on their experimental results, they do not directly test or attempt to disprove this hypothesis. Hence, this statement remains just that, an untested hypothesis.	
10	In Situ Observations of Nanoparticle Early Development Kinetics at Mineral—Water Interfaces	Iron oxide nanoparticles were prepared in water from a solution of ~0.1 mM $Fe(NO_3)_3$ at 1, 10, and 100 mM $NaNO_3$ at pH 3.6. The heterogeneous nucleation and growth of the iron oxide particles on a quartz surface were studied. The quartz surface was chemically and mechanically polished to an approximate roughness of 2.5 Å. The formation process was studied by simultaneous SAXS/GISAXS.	The authors used simultaneous SAXS/GISAXS to try and separate heterogeneous and homogeneous nucleation. They found that "the amount of homogeneously formed nanoparticles increased with increasing [ionic strength] and leveled off at 10 mM [ionic strength] and above"[41]. The reasoning behind these results is based on electrostatic repulsive forces. Furthermore, the observed smallest nanoparticle radii, at $[NaNO_3]$ = 1 and 10 mM, were 1.7 ± 0.3 nm and 1.8 ± 0.2 nm, respectively. Meanwhile, at the same $[NaNO_3]$, CNT predicted sizes of 21.1 and 31.5 nm. Finally, in Figure 5 within the paper[41], the authors present their proposed mechanism for the nucleation and growth behavior on the quartz surface.	*Importantly and quantitatively*, this paper demonstrates the inapplicability of CNT to a nanoparticle formation system. The authors have presented their "mechanistic and morphological understanding"[41], but have not provided any kinetics analysis to support their claim. The rigorous kinetics data has been collected, but no differential equations have been written for the nucleation and growth processes.	41
11	Nucleation and Growth of Metal Nanoparticles during	Palladium and rhodium nanoparticles were prepared from their metal-chloride salts in aqueous ethanol, in the	The authors claim their analysis of the SAXS measurements "[show] that the mechanism underlying the formation of metal nanoparticles in the photoreduction	The authors have collected excellent synchrotron data and have specifically recognized the importance of increased time resolution at the early times of particle	42

	Photoreduction Using In-Situ Time-Resolved SAXS Analysis	presence of PVP and benzoin, and reduced by photoirradiation. The reaction was monitored by in situ time-resolved SAXS and ex-situ TEM.	process is constituted of three elementary phases: 'autocatalytic reduction—nucleation', 'nucleation—growth', and 'diffusion-limited Ostwald ripening-based growth'."[42] Furthermore, the authors concluded that "increased time resolution enables one to understand the nucleation and growth process at the beginning of the formation reaction, and it facilitates the evaluation of the kinetics of elementary steps to provide a complete quantitative description of nanoparticle formation processes in the near future."[42]	formation studies. However, there are numerous cases of scientific missteps and confirmation bias in this paper. First, the mathematical basis for their data analysis was LSW theory and classical nucleation, which has been shown to *not* be suitable for strong-bonding systems like metal nanoparticle formation. Second, the authors routinely claim to be "confirming" their hypothesis and mechanism with additional experiments, but they do not take into account other possible explanations or alternative hypotheses—that is, there is little attempt to disprove in this paper. Third, the words used to describe their 'mechanism' (cited in the column to the left) are not well supported. Overall, the authors have collected excellent, commendable data. But, they do not analyze it appropriately, for example by taking disproven theories and applying them to their system. The authors did not determine the reaction stoichiometry for their system nor the (pseudo) elementary steps applicable to their particle formation reaction.	
12	In Situ UV/Vis, SAXS, and TEM Study of Single-Phase Gold Nanoparticle Growth	Gold nanoparticles (Au NPs) were prepared following the Stucky method.[43] Specifically, $(P(Ph)_3)Au^{I}Cl$ was reduced in toluene using the mild reductant, *tert*-butylamine-borane. The authors investigated the formation of Au NPs by UV-vis, SAXS, and TEM. Size versus time data were collected using SAXS and TEM, whereas volume fraction versus time was reported using UV-vis.	Depending on the conditions, the authors report an average particle diameter between 4.0 and 6.0 nm, with a best polydispersity of 7%. The TEM and SAXS data agree within experimental error. The particle formation process is reported by the authors to occur in four stages: (1) "early NP formation by the borane reaction is consistent with CNT. NP growth starts via a fast nucleation event of small clusters"; next, (2) Ostwald Ripening occurs "up to a critical particle radius. However, once particles reach this critical size—and, therefore, a critical surface energy—the mechanism	The strength of this study is that the authors have done a commendable job of using several direct techniques to collect kinetics data on their system. Unfortunately, the authors state that "the underlying mechanism is based on Ostwald ripening (OR), where the reaction kinetics is described with LSW theory."[44] However, the authors also note that the LSW kinetic model "only qualitatively describes the overall growth process and does not capture the discontinuity in dr/dt."[44] If true, then it follows that the full, correct formation mechanism cannot be described as claimed using LSW. What is missing from this work are the steps	44

			changes."; (3) "excess Au(0) monomers present in the solution, and apparently stabilized by the alkyl thiol molecules, react directly with the NP surface"; and finally, (4) "termination of NP growth when the concentration of Au(0) monomer is in equilibrium with the size of the existing Au NPs."[44]	of: (i) writing out the (pseudo) elementary steps for each possible mechanism, (ii) writing down the corresponding differential equations for each mechanism, and then (iii) attempting to fit the kinetics data—which mechanisms can be ruled out? Which fit the data? None of these key steps underlying a reliable mechanism have been done in this study.	
13	In Situ Small-Angle X-ray Scattering from Pd Nanoparticles Formed by Thermal Decomposition of Organo-Pd Catalyst Precursors Dissolved in Hydrocarbons	Palladium nanoparticles were prepared from solutions of either $Pd(acac)_2$ or $Pd(acetate)_2$ in toluene via the heat-up process, whereby the reaction solution was heated to 150 °C and 190 °C, respectively. The nanoparticle formation process was monitored using synchrotron SAXS. Independent repeat experiments were performed and monitored by TEM, XANES, and X-ray PDF analysis. Complete kinetics data were not reported.	The authors report a final size of 4.1 ± 0.1 nm for the particles formed from the precursor $Pd(acac)_2$. However, the particle size distribution in Figure 5 of the paper[45] suggests the size is much greater than ±0.1 nm, likely between ±1.0 - 1.5 nm. The SAXS and XANES data are in agreement with each other. Larger particles are observed at higher temperature, which the authors claim is due to "the additional thermal energy [that] should help marginally break Pd-ligand bonding."[45] Models were presented to describe the growth process of the two palladium systems.	The authors present high-quality synchrotron data. They have not attempted to overinterpret their data beyond qualitative models. However, they end their discussion section by saying that the "two different models can be used to interpret the growth patterns of the particles in $Pd(acac)_2$ and $Pd(acetate)_2$ toluene solutions".[45] No direct evidence supporting their cartoon drawings, presented as models, are provided. Missing are the pieces and steps to a reliable mechanism of determining the balanced chemical equation corresponding to their synthesis, collecting the needed kinetics data, postulating alternative mechanistic hypotheses, and the key step of determination of the (pseudo) elementary reactions that constitute the proposed mechanism.	45
14	Effect of Surfactant Concentration and Aggregation on the Growth Kinetics of Nickel Nanoparticles	Nickel nanoparticles were prepared from $Ni(acac)_2$, oleylaminne, and trioctylphosphine (TOP) with H_2 (g) as the reductant. The reaction was rapidly heated to 200 ºC, and the reaction time zero began once the temperature reached 200 ºC. Syntheses with	The authors report four time-resolved experiments at 0.5, 1.0, 1.0, and 2.0 molar equivalents of TOP to Ni(II). Based on the SAXS results, they were able to determine volume of particles, particle radius, and dispersion, all with respect to time. Hence, time-resolved size distributions could be reported for each of the four experiments. Next, the authors	The authors of this study have collected outstanding SAXS data and performed excellent, commendable initial analysis of the data. Next, the authors report fascinating results, particularly for samples (D) and (E), which are reported to both have TOP/Ni ratios of 1.0. Yet, the two samples display quite different kinetics.	46

		varying molar equivalents of TOP were investigated. The reaction was studied by SAXS. Nanoparticles were characterized, after the reaction had finished, by ex situ HR-TEM.	analyzed the growth kinetics for the reaction. "The growth mechanism was reported to occur in two stages: first nucleation by a continuous reduction which keeps the process far from the solution's monomer supersaturation point."[46] Then, in 'phase 2', "fast autocatalytic decomposition of the metal precursor on the nanoparticles' surfaces, promoting growth at the particle surface."[46] Next, "once there is a sufficient number of particles with a radius larger than the critical radius for forming ferromagnetic particles (approximately 7.5 nm), the particles start to aggregate through magnetic attraction. This is phase 3."[46] Finally, "[i]n phase 4, large aggregates settle out of solution, evidenced by a decrease in the total volume of particles."[46]	The authors have fit all of their data with the FW 2-step mechanism, which fits well until there is precipitation, or "settling" as the authors refer to it. It is clear that in all of the samples there is continuous nucleation and autocatalytic surface growth, as the kinetics data are well fit well with the integrated rate law corresponding to the two pseudo-elementary steps of the 2-step mechanism. However, the claims concerning 'phase 3' and 'phase 4' are not substantiated by the kinetics analysis provided. The exact composition of the nanoparticle surface after the reaction remains to be analyzed, and the exact products being formed have not been—but need to be— definitely determined. Overall, however, a noteworthy study that is recommend reading.	
15	Time-Resolved, in Situ, Small- and Wide-Angle X-ray Scattering To Monitor Pt Nanoparticle Structure Evolution Stabilized by Adsorbed $SnCl_3^-$ Ligands During Synthesis	Platinum nanoparticles coated with inorganic $SnCl_3^-$ ligands were synthesized in 7.5 M HCl, with excess Sn-ligand at 106 ºC. Reaction progress was monitored using SAXS and WAXS. Additional, ex situ, measurements were performed using EXAFS.	The authors used in situ SAXS and WAXS "to monitor the dynamic evolution of nanoparticle size and structure during the autoreduction of Pt-Sn complexes."[47] They observed an induction period, followed by a "burst generation of Pt primary particles", then a growth period.[47] The authors claim they are observing a "LaMer-type growth by primary particle diffusion."[47]	The authors have studied an intriguing Pt-Sn system and have collected impressive, high-quality SAXS and WAXS data. However, their data analysis has not taken into account any alternative hypotheses and states contradictory phrases. First, the authors claim that their kinetics data show a burst of nucleation, yet they see an induction period characteristic of slow, continuous nucleation and then autocatalytic growth—in essence disproving the LaMer model of putative "burst" nucleation and "diffusion-controlled" growth that they say applies to their data. Relevant here is that a comprehensive look at the literature claiming the LaMer model shows no	47

				compelling experimental support even in 70 years for that model. [12,13] Additionally, no alternative hypotheses have been disproven en route to the authors' conclusions. If the authors had attempted to *fit their kinetics data including its induction period,* then, in our opinion, they very likely would have disproven the applicability of the LaMer model and their subsequent diffusion-controlled growth conclusion. In short, the data analysis needs further study.	
16	Mesoscale Effects in Electrochemical Conversion: Coupling of Chemistry to Atomic- and Nanoscale structure in Iron-Based Electrodes	A series of iron compounds with differing amounts of oxygen and fluorine were studied. The compounds were as followed: Fe_2O_3, FeO, FeF_2, FeF_3, and $Fe^{II}_{(1-x)}Fe^{III}_xO_xF_{(2-x)}$, x = 0.5, 0.6. The synchrotron-based technique of SAXS and then PDF analysis were used to characterize the compounds.	The authors claim that "by combining PDF and SAXS, [they] can understand the link between chemistry and structure across multiple length scales."[48] While they did not study the mechanism of formation, the primary insight gained is that "the formation of unusual nanostructures in the mixed anion phases, without an interconnected network of Fe nanoparticles, may be attributed to the competitive growth of Fe nanoparticles nucleated in different anion environments, with different defect concentrations."[48] The authors also found that the defect level is only loosely correlated to the particle size. Instead the authors found that the composition of the precursor substrate to be a bigger indicator, where they hypothesize that increasing the reaction temperature would likely decrease the concentration of defects due to increased restructuring or annealing.	While the study is not explicitly about the mechanism of particle formation, it does produce high-quality synchrotron data on an interesting system, data of the type of interest to and needed by the nanoparticle formation community.	48
17	Resolving Early Stages of Homogeneous Iron(III)	Iron oxide clusters were prepared using a stopped-flow system with three injection lines containing: $Fe(NO_3)_3$, HNO_3,	The authors conclude that "the mechanism of FeO_x formation from 1 mM $Fe(NO_3)_3$ at pH 3 can be described by" four steps.[49] The four steps are: (i)	The authors have collected generally outstanding SAXS data. That said, they do not have the sensitivity in their	49

	Oxyhydroxide Formation from Iron(III) Nitrate Solution at pH 3 Using Time-Resolved SAXS	and pH 3 buffer with NaOH, respectively. The reaction was monitored by SAXS over approximately the first 1000 seconds. In addition, TEM and DLS measurements were obtained at different times. The majority of kinetics data were analyzed between 0 – 300 seconds.	"rapid (<1 s) polymerization reactions between multiple monomeric Fe hydrolysis species"; (ii) "formation of low dimensionality and/or polydisperse primary particles from 1 to 10 s after formation that evolve through a predominantly cluster-cluster addition mechanism to yield larger primary particles"; (iii) "ongoing growth of primary particles through a monomer addition mechanism…from 10 to 300 s to yield colloidal primary particles with radii of 3–10 nm"; and (iv) "aggregation (most likely reaction-limited) of colloidal primary particles through a cluster–cluster addition mechanism from 20 to 300 s to yield secondary particles with radii of gyration from 25 to 40 nm".[49]	system to monitor nucleation—and, instead. have claimed that nucleation is 'instantaneous' (occurring in <1 second). This of course seriously hinders experimental investigation of the true particle formation mechanism—instantaneous nucleation having been thoroughly *disproved*.[12,13] The authors have concluded that their findings "are generally consistent with previously developed general models for FeO_x formation" and "provides further understanding of the mechanisms of FeO_x formation and transformation."[49] Yet, these statements from their Conclusions are not supported by their results which do not provide new insights into the field of FeO_x formation. Instead, their discussion of 'mechanism' is entirely based on the literature and *not* their data. Their particular FeO_x formation system is complex and does not yield a well-determined, balanced reaction stoichiometry. The authors are also unable to write out the (pseudo)-elementary steps for their particle formation reaction. Overall, the primary contribution of this study is *excellent* SAXS growth data. But, a reworking of the analysis and conclusions from this work are in order, in our opinion.	
18	In Situ Probing Calcium Carbonate Formation by Combining Fast Controlled Precipitation Method and Small-Angle X-ray	Calcium carbonate ($CaCO_3$) clusters were formed from aqueous solutions of $Ca(HCO_3)_2$ at pH 5.2–5.5 with bubbling CO_2. Solutions were filtered through a 0.45 micron filter to remove dust. Reaction solutions were stirred at 850 rpm to	Based on their results, the authors conclude the precipitation process takes places in two 'domains'. "The first domain, called domain 1, is a metastable one…which could correspond to a prenucleation stage. The second domain called domain 2…is dominated by a rapid precipitation process."[50] The two	Overall, the authors have presented a fascinating, valuable study of the formation of $CaCO_3$ clusters. Impressively, they have presented the complete mass- and charge-balanced reaction. Further, they have collected kinetics data at different precursor	50

	Scattering	decrease CO_2 concentration, raise the pH, and initiate precipitation of $CaCO_3$. The reaction started with either $[Ca^{2+}]$ = 200 mg/L or 100 mg/L, both at 30 ºC. The reaction was monitored by synchrotron SAXS and resistivity.	methods, SAXS analysis and volume fraction of formed calcium carbonate as determined from the resistivity curve, were shown to be in agreement.	starting concentrations, and they have studied their reaction with multiple physical handles. The intent of the work is to provide evidence for the presence of prenucleation clusters and provide a proof of concept for their SAXS, pH, and resistivity techniques—mission accomplished. The study of $CaCO_3$ presented here is intriguing and deserves further investigation. Needed are a deeper kinetics and mechanistic investigation into the nucleation and growth processes of this interesting system and by the methods used, en route to a pseudo-elementary step based, proposed mechanism where at least several alternative mechanisms are tested and, ideally, disproved.	
19	*In situ* investigation of two-step nucleation and growth of CdS nanoparticle from solution	Cadmium sulfide nanoparticles were prepared using a free-jet setup to combine aqueous solutions of Na_2S and $CdCl_2$ in a micro mixer. SAXS and WAXS data were collected at different reaction times by moving the positions of the monochromatic X-ray beam and related by the expression $t_{react} = d/v$, where d is the distance to the mixing point and v is the flow velocity. Additional controls using DFT were performed with the Gaussian03 program package and the basis set HF-DGDZVP.	The authors collected data at four reaction times (150, 290, 530, and 1000 μs) and three jet velocities (10.6, 21.2, and 31.8 $m^1\ s^{-1}$). Based on their SAXS/WAXS experiments, the authors proposed a two-step formation mechanism of (i) nucleation of clusters and (ii) coexistence of nucleation and diffusion driven growth. They claim "this first nucleation process is driven by diffusion of the cadmium and sulfur ions and further nucleation continuously takes place in the regions of the interfaces of turbulent mixing. From these primary clusters larger particles develop."[51] From here, the authors claim the growth is by agglomerations of clusters and not by atomic, monomer attachment. Of note, the authors cite that "after 2.5 ms the median of the particle diameter of the growing population has reached a value of about 5 nm."[51] Finally,	The authors have presented an impressive, commendable experimental approach, especially on an important but difficult quantum dot system. That key positive so noted, the data do not support the overall conclusions, certainly not the paper's claim to have direct experimental *proof* of a nucleation *mechanism.* Not only is such proof impossible—one disproves instead[10,11]—the authors admit that their data are limited by early time sensitivity issues. No kinetics data are fit by a differential rate equation to *experimentally test* the proposed mechanism. No direct, experimental evidence is given for the Kinetically Effective Nucleus. With regard to the four criteria for a reliable mechanism detailed in the main text, the authors have only partially satisfied two	51

			based on their data, and their quantum calculations suggesting a structural prenucleation cluster model of $Cd_{13}S_4(SH)_{18}$, the conclude their study provides "direct experimental proof of a 2-step nucleation process for the very early stages of CdS formation and growth."[51]	of those requirements: they have collected kinetics data and mostly, but not completely, determined the reaction stoichiometry. Hence, additional work and data analysis are needed on this interesting system before reliable mechanistic conclusions can be claimed to be in hand.	
20	Colloidal nanoparticle size control: experimental and kinetic modeling investigation of the ligand–metal binding role in controlling the nucleation and growth kinetics	Palladium nanoparticles were prepared from Pd(II) acetate and either pyridine or toluene. Then, a mixture of TOP (trioctylphosphine) and 1-hexanol was added, the solution heated to 100 ºC, and stirring initiated. Characterization was done by STEM. Kinetics data was collected using *in situ* SAXS.	The authors constructed a ligand-based model to fit their kinetics data consisting of 4 steps: (1) A $\rightarrow$ B; (2) A + B $\rightarrow$ 2B; (3) A + L $\rightleftharpoons$ A•L; and (4) B + L $\rightleftharpoons$ B•L. This model was used to successfully fit the *in situ* SAXS kinetics data and provide mechanistic insights into the Pd nanoparticle formation process. The paper's results "demonstrate that the binding of ligands with both the metal precursor and nanoparticles surface kinetically controls the rates of nucleation and growth and as a result the duration of their overlap."[52]	The report by the Karim Group is an illustrative case, which is covered in detail in the main text, for how one *should approach* kinetics and mechanism in particle formation reactions. Karim and coworkers wrote out the proposed pseudo-elementary steps, obtained quantitative kinetics data, used more than one observable, and disproved alternative hypotheses. While the exact speciation of the Pd precursor is not exactly known, this and the limitations of their model are stated upfront. This paper is highly recommend reading for anyone conducting nanoparticle formation mechanistic research, especially when an excess of good binding ligand is present.	52
21	Mild Homogeneous Synthesis of Gold Nanoparticles through the Epoxide Route: Kinetics, Mechanisms, and Related One-Pot Composites	Gold nanoparticles were prepared using tetrachloroauric acid in aqueous glycerol solution. PVP or CTAC was used as a stabilizer. Kinetics data were collected using UV-Vis, SAXS, and pH. Resultant nanoparticles were characterized by TEM. The reaction was run at 25 °C for 1000 min. A final experiment was run on the formation of	The authors claim to have a new methodology for obtaining gold nanoparticles. They use the controlled hydrolysis of glycidol to steadily release OH^- to alkalize the solution until the pH reaches ~10 and reduced Au^{III}. The authors directly monitored the pH, conductivity, and UV-Vis absorbances at 315 and 400 nm as a function of reaction time. The in situ SAXS and ex situ TEM are shown to be in agreement.	The authors have carefully investigated a new method for synthesizing gold nanoparticles in an aqueous glycerol solution. They have not yet determined the complete stoichiometry of the reaction. Primarily, they have investigated the glycerol to glycidol process, and they have characterized the final product. The authors collected kinetics data following the overall reaction from *n* Au(III) to $Au(0)_n$. The possible pseudo-elementary steps have	53

		gold nanoparticles in an Al-hydrogel formed from $AlCl_3$ and glycerol.		not been hypothesized yet, but the authors note that they are not claiming a mechanism. Instead, they offer potential next steps as well as kinetic and mechanistic studies one could do to investigate the mechanism of formation for gold nanoparticles using the synthetic method investigated.	
22	Insights into the Formation Mechanism of CdSe Nanoplatelets Using in Situ X-ray Scattering	Two-dimensional CdSe nanoplatelets (NPLs) were prepared using a heating up procedure. A mixture of cadmium oleate, cadmium acetate, and trioctylphosphine-selenide was heated to between 170-200 °C. SAXS and WAXS were used to monitor the NPL formation.	The authors provide experimental data for the formation of 3 monolayers thick CdSe NPL via a heating up and one-pot procedure. The reaction was monitored from 0 to 2250 s where at least 3 different processes were observed. The data disproved "a templating effect or an oriented attachment formation mechanism."[54] The data were consistent with lateral growth of NPLs from a small number of initial seeds. These data were also consistent with previous studies done by the authors with a UV-vis probe[55] and a recent kinetic pathway proposed by others.[56]	The authors have presented a fascinating study on the formation of CdSe NPLs. First, their kinetics data are direct and high-quality. Next, these authors have applied a disproof-based method to the presentation of their results. They were careful not to claim more than the data revealed and address all possible hypotheses. With further experiments, the authors will be able to determine the complete reaction stoichiometry and the pseudo-elementary steps. Regardless, we recommend this paper for its excellent kinetics data and approach to experimental investigation!	54
23	Growth of Perovskite $CsPbBr_3$ Nanocrystals and Their Formed Superstructures Revealed by In Situ Spectroscopy	$CsPbBr_3$ perovskite nanocrystals (NCs) were prepared using the hot-injection technique. A solution of $CsCO_3$ and oleic acid was injected into a hot solution of $PbBr_2$, 1-octadecene, oleic acid, and oleylamine at 180 °C. The reaction was quickly quenched using an ice bath. The synthesis was followed using in situ photoluminescence. The nanocrystals were characterized using TEM and STEM. Finally, SAXS and WAXS were used to	The authors found two PL peaks during the synthesis of their $CsPbBr_3$ nanocrystals. The first appeared immediately at ~515 nm and was attributed to the formation of their $CsPbBr_3$ nanocrystals. The second appeared ~20 s after the start of the reaction at a red-shifted positon of 529 nm and was attributed to the SCs. SAXS and WAXS measurements, taken immediately after the synthesis, revealed the spontaneous formation of SCs on a disordered lattice. The authors "proposed a qualitative model for the perovskite NC growth via a self-size-selection process	The authors have provided an intriguing study on the in situ formation of $CsPbBr_3$ nanocrystals. In general, hot-injection reactions are notoriously difficult to monitor. The authors here have demonstrated the use of PL as a method to collect kinetics data on the formation process. Furthermore, they have identified that the growth process is complex between the growth of NCs to the formation of SCs and have hypothesized an initial qualitative model. Overall, the authors have provided the scientific community with the building blocks to study the	57

		monitor the distribution and arrangement of the nanocrystals into superstructures, or supercrystals (SCs), after the synthesis.	where only high-quality NCs assemble to the SC."[57]	mechanisms of perovskite nanocrystal formation. With continued efforts like this study, there is great potential that our understanding of perovskite nanocrystal formation will soon catch up with our understanding of metal nanoparticle formation.	
24	A comprehensive study of the crystallization mechanism involved in the nonaqueous formation of tungstite	Tungstite nanostructures were synthesized from WCl_6 in benzyl alcohol at 100 °C for 24 h. The resulting green-yellow powders were characterized by SEM, TEM, HR-TEM, XRD, and in situ SAXS measurements.	The authors monitored the formation of tungstite using TEM and SAXS. From their TEM, they report the fast formation of particles, the slow growth into cylinders, and then exfoliation into platelets. This general scheme is supported by their SAXS and XRD data.	The authors have thoroughly investigated this (seemingly) simple system and have shown "how elaborate the investigation of just one system can be and how many *ex* and *in situ* techniques have to be applied to monitor both the organic and inorganic processes."[58] While we analyze this paper in more detail in the main text (Section 4.3), the authors have presented a fascinating case of growth that evolves from spherical particles, to 3D cylinders, and finally 2D nanoplatelets.	58

Table S3. Summary of Papers Using XAFS to Collect Kinetics Data.

Entry	Title	System & Techniques Used to Monitor the Kinetics	Results and Proposed Chemical Mechanism	Conclusions, Insights, and Critical Analysis	Ref.
1	Structural Analysis of Polymer-Protected Platinum/Rhodium Bimetallic Clusters Using Extended X-ray Absorption Fine Structure Spectroscopy. Importance of Microclusters for the Formation of Bimetallic Clusters	Platinum/Rhodium bimetallic clusters were prepared from aqueous solutions of $RhCl_3$ and H_2PtCl_6. PVP was used a protecting polymer in the aqueous/ethanol metal solutions. The reaction solution was stirred and refluxed at 100 °C for 2 hours under N_2. Reactions were run using 1:1, 4:1, and 1:4 ratios of platinum:rhodium. Clusters were characterized using TEM, STM, and EXAFS.	The authors found by STM and TEM "that the cluster particle is composed of several small microclusters, less than 10 Å in diameter".[59] To investigate this finding, the authors used EXAFS in order to better determine the structure and composition of the clusters and microclusters. They found direct EXAFS evidence of small, Rh_{13} microclusters, which were corroborated by STM. As the reaction continues, the microclusters aggregate together and "serve as building blocks for pseudo-close-packed superstructures."[59]	The authors have presented fascinating, early EXAFS data for the observation of small, less than 1.0 nanometer, sized clusters of strong-bonding metal nanoparticles. They have not proposed any chemical mechanism for the nucleation or growth of the Pt/Rh bimetallic clusters, but rather just present the data they were able to collect. Then, they only proposed the possible pathways based on the data collected, known thermodynamics, and other literature available at the time—a cautious, commendable approach that sets the stage for detailed kinetics and mechanistic studies on this classic PVP stabilizer, aqueous/alcohol reductant, bimetallic Pt/Rh particle formation system.	59
2	Genesis of Pt Clusters in Reverse Micelles Investigated by in Situ X-ray Absorption Spectroscopy	Platinum nanoclusters were synthesized from H_2PtCl_6 inside of AOT reverse micelles, where AOT = sodium bis(2-ethyl hexyl) sulfosuccinate. The microemulsion system was prepared in a mixture of *n*-heptane and water. Platinum was reduced using hydrazine (N_2H_4). The reaction was monitored using XAFS, and the particles were visualized using TEM.	The authors monitored the Pt L_{III}-edge with increasing concentration of N_2H_4. The authors claim to observe "six distinguishable steps…for the formation of Pt clusters at the early stage."[60] These steps include a reduction reaction from Pt^{4+} to Pt^{2+}, ligand exchange from $PtCl_4^{2-}$ to $Pt(OH)_4^{2-}$, a further reduction reaction from Pt^{2+} to Pt^0, and then particle growth. All the steps are found to be a function of the hydrazine concentration. Furthermore, the authors claim that the TEM micrograph "shows that the size distribution of the clusters is monodisperse."[60]	The authors have produced high-quality XAFS data but have not analyzed it in a way or at a level that can produce reliable mechanistic insights. First, the authors have not determined the complete mass and charge balanced reaction. Second, they have not produced the kinetics (concentration versus time) data needed to test proposed mechanisms by attempted fits to that data. Additionally, no disproof of alternative mechanistic hypotheses is provided.	60

3	Aggregated structure analysis of polymer-protected platinum/ruthenium colloidal dispersions using EXAFS, HRTEM, and electron diffraction measurements	Platinum/ruthenium colloidal dispersions were prepared from hexachloroplatinic(IV) acid in water combined with ruthenium(III) chloride in ethanol. PVP was added to the 1:1 ethanol:water mixture. The solution was refluxed at 100 ºC for 2 hours under atmospheric air with a subsequent control conducted under nitrogen. The colloidal dispersions were characterized by ex situ HR-TEM, EXAFS, and electron diffraction.	The authors characterized the Pt and Ru colloids separately, as well as combined. From EXAFS, the author report that "the aggregation occurs between small monometallic Pt clusters (diameter ca. 15 Å) and partially oxidized Ru microclusters (diameter less than 10 Å)."[61] It was concluded that a Pt/Ru alloy was not present in colloidal dispersion. The authors state that "an agglomerate, with more than 50 Å in diameter, consists of several partially oxidized Ru microclusters and small monometallic Pt clusters, not consisting of Pt/Ru alloyed clusters."[61] For platinum, it is most likely that 3 to 4 clusters of Pt_{55} are present, whereas, for ruthenium, the microclusters are likely Ru_{13}.	The authors have expertly used EXAFS in order to extract direct, valuable information on the particle synthesis. This system is, therefore, ripe for the design of appropriate kinetics and other experiments that can lead to a reliable mechanism for this mixed metal system.	61
4	Formation Mechanism of Pt Particles by Photoreduction of Pt Ions in Polymer Solutions	Platinum nanoparticles were prepared from $H_2PtCl_6 \bullet 6H_2O$ in aqueous ethanol with PVP. Solutions were bubbled with N_2 to remove dissolved O_2. Particles were prepared by irradiating dilute (0.66 mM) or concentrated (9.65 mM) solutions using a 500 W super-high-pressure mercury lamp. Characterization was done using UV-vis and TEM. In situ measurements were carrying out by EXAFS of the Pt L_3 edge.	Based on the EXAFS and XANES analyses, the authors propose the formation mechanism for Pt particles in this system to be "the following steps: (1) reduction of $PtCl_6^{2-}$ to $PtCl_4^{2-}$, (2) dissociation of Cl from $PtCl_4^{2-}$, followed by reduction of Pt^{2+} ionic species to Pt^0, (3) formation of a Pt^0–Pt^0 bond and particle growth by the association of Pt^0–Pt^0."[62] Aging experiments, where particles after irradiation were allowed to sit for 24 hours in the dark, with and without PVP revealed that PVP is needed to stabilize particles. Without PVP, particles agglomerated over the 24-hour, dark period.	The authors of this study have collected excellent XAFS data and have investigated the importance of using the stabilizer PVP for the long-term stability of their particles. The authors additionally have identified important *qualitative* trends in the appearance or disappearance of platinum species, Pt^{4+}, Pt^{2+}, and Pt^0 and proposed pseudo-elementary steps have been written out for this reaction. Missing and hence possible targets for future research are: writing differential equations corresponding to the proposed pseudo-elementary steps, collecting kinetics data, and then testing the proposed mechanisms by attempting *quantitative fits* to each proposed mechanism, all in a disproof-based manner.	62

5	In Situ XAFS Studies of Au Particle Formation by Photoreduction in Polymer Solutions	Gold nanoparticles were prepared from $HAuCl_4 \bullet 4H_2O$ in aqueous ethanol with PVP. Solutions were bubbled with N_2 to remove dissolved O_2. Particles were prepared by irradiating dilute (0.66 mM) or concentrated (12.2 mM) solutions using a 500 W super-high-pressure mercury lamp. Characterization was done using UV-vis and TEM. In situ and ex situ measurements were carrying out by XAFS.	UV-vis measurements at 545 nm reveal the formation of gold nanoparticles over the course of 10 hours with a peak growing in as early as 15 minutes. By XAFS, only three gold species were present through the reaction, Au^{3+}, Au^{+}, and Au^{0}. Based on the XANES and EXAFS results, the authors proposed a 3-step formation mechanism. "(1) The bond of Au–Cl rapidly dissociates until the reduction time reaches up to 30 min."[63] "(2) During the reduction time of 30–360 min, the peak intensity of the Au–Cl bond gradually decreases with time, while the peak attributed to the Au^0–Au^0 metallic bond appears around 2.8 Å and its intensity increases with time."[63] "(3) On the prolonged photoirradiation (the reduction time longer than 360 min), $AuCl_2^-$ is completely consumed, and the growth process of Au metal particles is obviously observed despite the [coordination number]s remaining nearly constant."[63]	The authors have collected excellent in situ UV-vis and XAFS data. The Fourier transformed XAFS data have been presented, but not analyzed or interpreted at a quantitative level. The authors have done valuable *qualitative* analysis of their data, corroborated their analysis by TEM, and hypothetical reaction steps have been produced. Remaining to be done are: (i) writing out the experimentally supported pseudo-elementary steps for their proposed mechanism; and (ii) *fitting* their kinetics data to the proposed mechanism(s), all in a disproof-based fashion so as to lead to more reliable mechanistic conclusions.	63
6	In Situ Time-Resolved XAFS Studies of Metal Particle Formation by Photoreduction in Polymer Solutions	Rhodium and palladium nanoparticles were prepared in aqueous ethanol solutions with PVP and benzoin (photoactivator) and studied by UV-vis, TEM, and in situ DXAFS. The starting metal salts were $RhCl_3 \bullet 3H_2O$ and $PdCl_2$. Solutions were degassed using N_2. Particles were formed by irradiation from a 500 W super-high-pressure mercury lamp.	By UV-vis, the loss of metal precursors is quantitatively monitored. Particle size distributions were determined by counting > 200 particles observed by TEM. Most importantly, in situ DXAFS measurements were collected for Rh and Pd every 36 and 40 seconds, respectively. In Scheme 1 of the paper,[64] the pseudo-elementary steps of the proposed mechanism were explicitly written out. Differential rate equations were derived from these pseudo-elementary steps and the kinetics data	Overall, this study[64] by Harada and Inada is a classic in the literature. The authors have collected excellent, direct kinetics data on the formation of Rh and Pd nanoparticles. They have successfully written out the pseudo-elementary steps, written differential equations for their reaction, and fit the data. They have corroborated these findings with a separate physical technique (UV-vis). The primary, still-needed experiment is the complete understanding of the reduction process,	64

			for both Rh and Pd were fit with those proposed steps. The authors report, "the reduction rate of Rh(III) aqua chloro complexes in PVP solutions was found to be slower than that of Pd(II)."[64]	starting with the balanced reaction. Does Rh(III) immediately reduce to Rh(0) or does it reduce to Rh(I) first? What species are formed in solution? What is the exact composition of the Kinetically Effective Nucleus (KEN) for $Rh(0)_n$ and $Pd(0)_m$? This classic metal-chloride plus aqueous alcohol reductant system merits further investigation as do the other aqueous alcohol reductant systems already mentioned.	
7	Insights into Initial Kinetic Nucleation of Gold Nanocrystals	Gold nanoparticles were synthesized from an aqueous solution of $AuCl_4$ with citric acid as the reductant, and PVP as a stabilizing polymer. The reaction was stirred and heated to 70 ºC, and the reaction was run for 260 minutes. Ex situ characterization was done by UV-vis and TEM. In situ QXAFS were collected at the Au L_{III}-edge using a peristaltic pump set-up.	Based on their QXAFS data, the authors have "propose[d] a kinetic three-step mechanism involving the initial nucleation, slow growth, and eventual coalescence for the Au [nanocrystals] formation."[65] The three-step mechanism was divided up into three stages. "Stage I can be considered as the initial nucleation step, exhibiting a faster process compared with stage II which stands for the growth step. In Stage III, however, $N_{Au\text{-}Au}$ increases quickly along with the decreased $N_{Au\text{-}Cl}$, indicating the rapid increase in size of Au [nanocrystals]."[65]	The authors have collected outstanding in situ synchrotron data. Their time resolved data is shown in their[65] Figure 2. The data presented there is an excellent example of what the field as a whole should be striving to collect, in our opinion. That said, the authors claim of a 'mechanism' for the nucleation of Au nanocrystals is premature. They have yet to derive the differential equations or fit their kinetics data based on their pseudo-elementary steps—only then will they be able to claim a more reliable mechanism. The language used in their[65] Figure 4 is proper in this regard where they claim just "[a] schematic representation of the formation process"[65] that *qualitatively* describes their system and its kinetics data.	65
8	In Situ Observation of Nucleation and Growth Process of Gold Nanoparticles by Quick XAFS Spectroscopy	Gold nanoparticles (AuNPs) were synthesized from $HAuCl_4$ in toluene with the addition of tetraoctylammonium bromide (TOAB) and dodecanethiol (DT). Then, a solution of	The authors found that, in the presence of 2 or more equivalents of DT, the gold precursor was reduced from Au^{3+} to Au^{1+}. At 1 molar equivalent of DT to gold, fifty percent of the gold was Au^{3+} fifty percent was Au^{1+}. The resulting	The authors have conducted a valuable study that includes a number of careful controls to characterize and determine the speciation of their starting reaction. Next, they collected excellent, direct synchrotron data on the transformation	66

		$NaBH_4$ in DMF was added. The reaction was studied by QXAFS. Characterization was done using XAFS, TEM, and UV-vis.	AuNPs were reported to be 3.3 ± 0.5 nm in diameter and covered with DT (as the surface ligand). The authors report that their "in situ analysis showed a different mechanism" (than what is typically cited/reported in the literature; e.g., often the LaMer model or the FW 2-step mechanism) "namely the reduction of all of Au ions, nucleation, and aggregation of the nuclei causing the particles to grow larger."[66] Most notably, the authors report direct XAFS data supporting the formation of a Au_4 cluster at 4.6 seconds after the addition of $NaBH_4$.	of Au^{3+} / Au^{1+} to AuNPs. These positives so noted, the authors claim of a 'new mechanism' is not substantiated by their present data. They have yet to determine the exact pseudo-elementary steps for the reaction nor use those to define the differential equations required to fit kinetics data—that also needs to be acquired. Additionally, disproof of all reasonable alternative mechanisms remains to be done. Such studies would be welcome on this AuNP formation system with its specific of Au, DT, and TOAB components.	
9	*In Situ* Au L_3 and L_2 edge XANES spectral analysis during growth of thiol protected gold nanoparticles for the study on particle size dependent electronic properties	Gold nanoparticles were prepared from a toluene solution of $AuCl_4^-$ and dodecanethiol. (Auric acid was neutralized by tetraoctylbutylammonium bromide, which then transferred the $AuCl_4^-$ into the organic-toluene phase from the aqueous.) $NaBH_4$ in DMF was used as a reducing agent. QXAFS were used to monitor the nanoparticle formation process with 100 millisecond resolution.	XANES data suggests that the reduction of Au^{3+} and Au^+ in solution to Au^0 occurs by time = 3.6 seconds. From there and based "on the average state of the absorption atom"[67] determined by XAFS, the "results suggested that [gold nanoparticles] grow via the aggregation of [gold nanoparticles] themselves. As a result, we can estimate the particles size from the fraction of surface atoms, or, in other words, the dispersion."[67] By the end of the reaction time, the authors have calculated a dispersion of 28.3 percent. Most compelling, the authors have observed, *in situ*, the formation of gold nanoparticles at *both* the L_3- and L_2-edges, and they have produced consistent, comparable results. No mechanism for the gold nanoparticle formation has been proposed, however.	The authors deserve to be commended for their impressive, high-quality QXAFS data. Remaining studies needed to obtain a mechanism for this interesting system include: (i) complete characterization of the precursor solution and resulting particles; (ii) proposing and testing plausible mechanisms of formation via their associated differential equations, all (iii) with an eye on a disproof- and Ockham's razor-based approach so as to yield a reliable, minimum proposed mechanism.	67
10	An *in situ* quick XAFS spectroscopy study of the formation mechanism of small gold nanoparticles	Gold nanoparticles were prepared from $HAuCl_4$ in DMF using the reductant $NaBH_4$ and in the presence of a passivant.	The authors collected time-resolved XANES and EXAFS. Their XANES suggest "that the size of Au nuclei is kinetically controlled by the speed with	The authors have presented a cartoon scheme for the "formation mechanism of gold nanoparticles."[68] The scheme is based off of the broad conclusions	68

	supported by porphyrin-cored tetradentate passivants	The two passivants used were: (**1**) α,α,α,α-5,10,15,20-(*o*-bisdisulfidepropylamidophenyl)-porphyrin and (**2**) 2,2'-dithiobis(*N*-(4-methyphenyl). Time-dependent studies of the gold particle formation were done using QXAFS. Further characterization was performed using UV-vis and TEM.	which the passivants trap the growing Au nuclei."[68] Their EXAFS analysis supports their XANES conclusions as the authors found "that **1** suppresses the particle growth more efficiently than **2** to provide smaller gold nanoparticles."[68] Furthermore, their end-time TEM reports smaller average size and narrow size distribution for Au nanoparticles formed in the presence of passivant **1**, than for passivant **2**. Overall, the authors conclude "the size of the Au nuclei is kinetically controlled."[68]	determined from the (time-resolved) QXAFS data. Unfortunately, the authors have not defined the exact stoichiometry or derived the kinetics, so their proposed scheme for gold nanoparticle formation is *not* a mechanism. It is just a proposed reaction scheme. It is worth noting that the authors have good kinetics data, and they have completed a number of well thought out controls, but the authors have not performed a rigorous mechanistic analysis.	
11	*In situ* XAFS experiments using a microfluidic cell: application to initial growth of CdSe nanocrystals	CdSe nanocrystals were synthesized by heating $Cd(CH_3COO)_2$, oleic acid, and octadecene (ODE) at 453 K under Ar using a microfluidic cell. Ligand, dodecylamine ($(CH_3(CH_2)_{11}NH_2$, DDA) in ODE, was added and the reaction solution was heated to 513 K. The reaction was monitored from 0.0 s to 8.1 s using XAFS, UV-Vis, and photoluminescence (PL).	The formation of $(CdSe)_n$ particles was observed by XANES, while simultaneously UV-Vis and PL spectroscopies were able to monitor the particle formation and crystallinity. Given the combined, XANES, EXAFS, UV-Vis, and PL results, the authors present preliminary insights into the initial formation of $(CdSe)_n$ particles.	The authors have presented a fascinating study and have keenly utilized a microfluidic device to probe the early time points of the reaction. Further, they have independently determined the Se-Cd coordination number three ways as a function of time. As we stated in the main text, further studies will allow them to (i) elucidate the exact reaction stoichiometry and (ii) write the complete pseudo-elementary steps for the particle-formation mechanism. These authors have already collected excellent kinetics data and incorporated disproof-based methods into their experimentation. Their study is, in our opinion, intriguing and a must-read.	69
12	Nucleation and Aggregative Growth Process of Platinum Nanoparticles Studied by in Situ Quick XAFS Spectroscopy	Platinum nanoparticles were prepared from either $H_2PtCl_6•6H_2O$ or K_2PtCl_4 in aqueous ethanol with PVP and benzoin. TEM was used to determine the average diameter of 200 particles. In situ QXAFS	The authors report that their "quantitative in situ QXAFS analysis" reveal "the mechanism underlying the formation of Pt nanoparticles in the photoreduction process of three elementary stages, reduction-nucleation, autocatalytic surface growth on	The authors of the study have collected excellent, direct kinetics data. They write out proposed pseudo-elementary steps, and they use the associated differential equations for fitting their data, specifically the FW 2-step mechanism of slow, continuous	70

		and data analysis are reported, along with UV-vis.	nucleates, and Ostwald ripening-based growth."[70] Kinetic rate equations have been written for the nucleation and growth steps. Then, the Ostwald ripening contribution is included with a "logistic 'turn-on' function to activate Ostwald ripening at a time τ_{OR}".[70] The LaMer model has been described as *not* applicable to this system.	nucleation and then autocatalytic surface growth. The authors also fit their data with the semi-empirical Avrami-Erofe'ye equation, although it is known not to yield mechanistic insights since balanced equations are not involved in such physical-chemistry models. Ostwald ripening is added along with a k_{OR} rate parameter as part of the fitting. Several areas of investigation are recommended for this system, including: (i) fuller investigation of the more intimate rate law for nucleation; (ii) the effect(s) of added ligand, including on agglomeration; and (iii) more evidence for or against Ostwald ripening vs Particle migration and coalescence, for example.	
13	Formation and oxidation mechanisms of Pd–Zn nanoparticles on a ZnO supported Pd catalyst studied by *in situ* time-resolved QXAFS and DXAFS	PdZn nanoparticles were prepared from ZnO substrate with Pd particles formed on the surface from $PdCl_2$ under basic aqueous conditions at 353 K and then calcined at 773 K. The result was a precipitate of 3 wt% Pd/ZnO. This was used under 20 kPa H_2 (reductive) or O_2 (oxidative) conditions at 673 K to form PdZn particles. Kinetics data was collected using in situ DXAFS measurements. Characterization was done using XAFS and XRD.	The two processes measured were: (1) the reduction of PdO on the surface of ZnO to Pd nanos and then PdZn; and (2) the oxidation of PdZn to Pd/Zn on ZnO and then PdO/ZnO on ZnO. The study demonstrated the direct monitoring of the full redox process of Pd/ZnO. The authors concluded that the "PdZn nanoparticles were formed on ZnO through a two-step scheme under a hydrogen atmosphere."[71] They found the initial reduction to be fast (< 1 s) and the formation of PdZn to be longer (> 10s of min). The authors for the two reduction steps and two oxidation steps to have single exponential, first-order rate constants. Based on their results, the authors proposed, as their Fig. 6, a "mechanism of the redox process of Pd/ZnO."[71]	The authors have worked on an intriguing system with important implications in the catalytic conversion of methanol. They have collected excellent time-resolved data. However, the balanced stoichiometry needed en route to a reliable mechanism has not been determined. The fitting of their data to a single, pseudo-first-order 'rate' equation is not explained nor is the equation used to fit their data explicitly reported in either the main text or the SI. Overall, the authors have not determined a *mechanism* yet report 'rates' for the 'steps' of their reaction scheme. Additional study of this system is both of interest as well as needed.	71

14	*In situ* time-resolved DXAFS study of Rh nanoparticle formation mechanism in ethylene glycol at elevated temperature	Rhodium nanoparticles were prepared from rhodium(II) chloride hydrate in ethylene glycol with PVP. The ratio of Rh:PVP were 1:15, 1:30, and 2:15. Kinetics measurements were collected using DXAFS at 403 K. Further ex situ measurements were done using ICP-MS and TEM.	XANES spectra, with near perfect isosbestic points, are reported for the formation of Rh nanoparticles. The formation process is suggested to be pseudo-first order in Rh^{3+} concentration. While some issues were reported in the discussion of the EXAFS results, the findings suggest that the nucleation process involves the formation of $(Rh^0)_n$, were n is small, n = 1, 2, or 3 Rh^0 atoms. The TEM micrographs display multipod nanoparticles, suggesting that aggregation of small particles may contribute to their formation, something that merits additional investigation. Based on the experimental evidence, the authors hypothesis the following word-based "mechanism" for Rh nanoparticle formation in ethylene glycol with PVP at 403 K: (1) "Rh^{3+} precursor might be thermally reduced by [ethylene glycol] to nucleate to be Rh^0 monomer"[16]; (2) "the Rh [nanoparticles] formed very rapidly to be uniform size [nanoparticles], which are stable under the reaction conditions"[16]; and then (3) "a repeat of the second step, which is the repeat of uniform Rh [nanoparticle] formation."[16]	The authors in this study have collected high-quality, direct XAFS kinetics data for the formation of Rh nanoparticles. They have defined pseudo-elementary steps for the formation process and produced a rate law for those steps. They have used multiple physical handles. Still missing and hence targets for future research include: the balanced reaction stoichiometry; fitting the kinetics data with the integrated form of the differential rate law; and a focus on achieving a disproof-based, minimum mechanism that can quantitatively explain all the observed data.	16
15	XAFS in the tracking of reactions in aqueous solution: a case of redox reaction between $[AuCl_4]^-$ complex ions and ethanol	Gold nanoparticles were prepared from the reduction of $AuCl_4^-$ in a basic ethanol solution (pH = 12) at 22.5 °C. The reaction was monitored using synchrotron XAFS.	The authors have presented a short summary of the benefits of using XAFS to collect kinetics data for gold particle formation in an aqueous medium. They have presented very nice kinetics data for the reduction process of Au(III) to Au(0). Finally, the authors have presented a net, balanced chemical reaction for the hydrolysis of $Au(OH)_4^-$	The authors illustrate the benefits of using XAFS to collect high-quality, direct kinetics data. Unfortunately, the authors chose to fit their data with an empirical first-order rate function that, thereby, produced a *single* rate parameter (that is not a rate constant, as it is not defined by a balanced reaction) that is unable to even	72

			to Au(0).	qualitatively describe the *two processes* of nucleation and growth. Hence, remaining to be accomplished are: (i) collecting the fuller experimental rate law; (ii) producing pseudo-elementary steps for their reaction with defined rate constants for each step that, overall, define their proposed mechanism; (iii) producing alternative mechanisms to also test, and (iv) testing all possible reasonable mechanisms by attempted fits to the full kinetics and rate law, all in a disproof-based, Ockham's razor obeying fashion.	
16	Insights into the Formation Mechanism of Rhodium Nanocubes	Rhodium nanocubes were synthesized at 130 ºC from $RhCl_3•3H_2O$ in ethylene glycol with tetradecyltrimethylammonium bromide (TTAB) and PVP. Direct formation kinetics data were collected using DXAFS. Ex situ measurements were performed using MALDI-TOF MS, XRD, TEM, and UV-Vis.	Kinetics data (concentration of precursor versus time) were monitored directly using XANES. They were fit with the FW 2-Step mechanism with A = Rh_0^{3+} and B = Rh_t^{3+}. Throughout the experiment, samples were collected and ex situ measurements were taken using MALDI-TOF MS, XRD, TEM, and UV-Vis to determine the speciation, ex situ reaction progress, and particle size distributions. Strong evidence was proposed for their 4-step mechanism: "(1) exchange of Rh^{3+} ligand sphere, (2) formation of Rh [nanocrystal] nuclei,…(3) evolution of nuclei into Rh [nanocrystals], and (4) shape corrections."[73]	The authors have presented an impressive study. Points of note include the: (i) collection of direct kinetics data; (ii) characterization of the reaction solution as a function of time; (iii) direct evidence of $Rh_{2\text{-}4}$ clusters—*an important finding suggestive of low molecularity nucleation*; (iv) fitting of the kinetics data to appropriate mechanistic equations; and (v) attempts to disprove alternative hypotheses. Additional experimental work that would be welcome includes (a) the temperature dependence of this classic system and study; and (b) attempted disproof of all reasonable alternative mechanistic hypotheses Nevertheless, as it stands this study is *one of the best studies* we have found that uses XAFS to collect kinetics data en route to a particle formation mechanism. As such, it is recommend reading in our opinion to anyone	73

				looking to use XAFS to study metal nanoparticle formation.	
17	Formation mechanism of metal nanoparticles studied by XAFS spectroscopy and effective synthesis of small metal nanoparticles	Gold nanoparticles were prepared chemically from tetrachloroauric(III) acid in DMF using $NaBH_4$ as the reductant. Resulting particles were stabilized with a series of thiol-containing ligands. The three types were: (i) tetradentate, (ii) monodentate, and (iii) dodecanethiol. The Au nanoparticle formation mechanism was studied by using QXAFS and TEM. Second, rhodium nanoparticles were prepared by photodeposition on TiO_2 in solution. The Rh nanoparticle formation mechanism was studied by using DXAFS, XPS, EDX, and TEM.	The authors found the syntheses that used the tetradentate ligand (containing 4 thiol groups) consistently produced smaller Au nanoparticles than the syntheses with either the monodentate ligand or the dodecanethiol. This was consistent across a range of S:Au ratios (0.1:1 to 16:1). From the XAFS data, the authors observe by 4.6 seconds into the reaction that all of the Au^{3+} and Au^{+} has been reduced to form Au^0 nuclei. The authors claim "the structure of the Au nuclei is estimated to be an Au_4 cluster."[74] From this, they propose the mechanism of gold nanoparticle formation is "the reduction of all of [the] Au ions, formation of nuclei, aggregation of the nuclei, and then the particles to grow larger."[74] For the Rh nanoparticle formation by photodeposition on TiO_2, the authors claim that "the in situ XAPS study suggested the photodeposition mechanism as followed; the Langmuir type adsorption of Rh^{3+} ions on TiO_2 to form Rh-O bonds; the reduction of Rh^{3+} ions to Rh metals on the surface of irradiated TiO_2; the constant appearance of Rh metal particles."[74] Furthermore, the deposited Rh nanoparticles were found to have abnormal morphologies due to interactions with the TiO_2.	The effectiveness of QXAFS cannot be overstated. The authors have compiled an impressive dataset for the formation of Au nanoparticles. Of particular note, the direct identification of the Au_4 cluster is an important result of significant value to the particle formation community, one that argues strongly against Classical Nucleation Theory in at least this example. The authors do claim that they have elucidated the mechanism of gold nanoparticle formation based on their direct observation of the reaction at different times. What remains to be done to support their claim of knowing the mechanism includes: (i) obtaining an experimentally based balanced reaction; (ii) writing down differential equation for their proposed mechanism(s); (iii) fit their high-quality kinetics data to each and every reasonable mechanism; and critically (iv) disproof of at least a couple, primary alternative mechanisms.	74
18	An *in situ* XAFS study—the formation mechanism of gold nanoparticles from X-ray-irradiated ionic liquid	Gold nanoparticles were prepared from the ionic liquid [BMIM][$AuCl_4$] at room temperature under hard X-ray irradiation (BMIM = 1-butyl-	The authors collected XAFS measurements at 30-90 minute intervals over 11.5 hours, at which the solution color had completely changed. At 5.5 hours, the authors observe an *N* ratio of	The authors have collected interesting, but limited, XAFS data. The paper is unfortunately rife with confirmation bias rather than the recommended disproof-based scientific approach. For	75

		3methylimidazolium). The reaction solution and the resulting particles were characterized by XAFS (both EXAFS and XANES analyses). TEM and XRD measurements were taken and reported in the SI.	1:2 and an $N_{Au\text{-}Au}$ value of 1.18, which they determine is evidence for "a structure like $Cl_2Au\text{-}AuCl_2$."[75] Based on their XAFS analyses, the authors propose a new "formation mechanism of gold nanoparticles" where the precursor $AuCl_4^-$ slowly loses Cl^- until the dichloroaurate complex dimerizes. The final particle is assumed to be stabilized in the ionic liquid by chloride.	example, the exact species in solution are not known, and considering ionic liquids, there are *numerous* speciation possibilities. The authors have used only simulations to "confirm" the existence of the $Cl_2Au\text{-}AuCl_2$ in solution as one example. Second, no kinetics data (concentration versus time) have been obtained nor fit with any proposed mechanism-based differential equation. Third, no corroborating evidence by any other technique is provided, be it in situ or ex situ, for the conclusions or proposed mechanism. It follows that the mechanistic claims in this paper need to be treated with considerable caution.	
19	An in situ X-ray absorption spectroscopy study of copper nanoparticles in microemulsion	Copper nanoparticles were prepared from copper sulfate hydrate and sodium borohydride in reverse micelles. The microemulsions were prepared as followed: oil phase of heptane; aqueous phase a mixture of butanol and cetyltrimethylammonium bromide. Four reactions were studied varying the percentage of aqueous phase, concentration of $NaBH_4$, and the reaction time. Characterization of the copper nanoparticles was done by XANES and EXAFS at the end of the reaction time.	The primary finding reported by the authors was that "the decrease in water content from 15% to 13% in the reverse micelles was concluded to produce a larger amount of metallic copper in these microemulsions with a radius slightly smaller than the metallic copper nanoparticles obtained in the reaction with 15% water."[76] They further report that the lower water content resulted in a slower reduction of copper.	The authors made several claims about the reduction reaction of copper and the formation of the copper nanoparticles that do not seem firm based on the experiments conducted. For example, the authors claim to have a detailed understanding of the reaction system, but have not done any other characterization experiments outside of the 4 XAFS data sets. The authors further claim that the copper disproportionates at long, 8 hours, reaction time versus 2 hours, but this claim is drawn from just two data points, and not continuous monitoring throughout the reaction time, and hence seems ill-supported. Overall, none of the 5 criteria for a reliable mechanistic study have been fulfilled for this copper nanoparticle formation system that need, therefore, considerable additional study.	76

20	Detection and characterization of sub-critical nuclei during reactive Pd metal nucleation by X-ray absorption spectroscopy	Palladium nanoparticles were prepared from $[NH_4]_2PdCl_2$ in water at the interface with an organic layer of ααα-trifluorotoluene containing the reducing agent ferrocene. The aqueous phase contained LiCl, and the organic phase contained [BTPPA][TFPB], bis(triphenyl-phosphoranylidene) ammonium and tetrakis[3,5-bis(trifluoromethyl)-phenyl]borate respectively, as supporting electrolytes. Time-resolved data was collected using QEXAFS in fluorescence-yield mode.	Depending on the initial concentrations of palladium and ferrocene, the authors claim to observe no nucleation, spontaneous nucleation and growth, or metastable states due to density fluctuations. The authors point to classical nucleation theory (CNT) literature to support their results as "CNT predicts a metastable pre-nucleation state with sub-critical nuclei or clusters in a dynamic equilibrium with solute monomers."[77] The authors find that their observation of 'sub-critical nuclei' are in line with recent investigations of Au nanoparticles that have a 'sub-critical nucleus' size of 25 ± 4 nm. Finally, the authors claim they have "provided evidence of the presence of sub-critical nuclei of Pd metal before a stable metal product is actually formed, as predicted by CNT."[77] A strength of this study is that numerous control experiments were conducted to ensure the synthesis at the interface between the organic and aqueous phases was not producing false XAFS results or that X-rays were induced artefacts.	The authors have a creative approach to the designed, controlled synthesis of palladium nanoparticles. Furthermore, they have collected direct, valuable XAFS data on the particle formation reaction. However, the application of CNT and its assumption of a 'critical sized nucleus' is not supported by their results—and is not consistent with other reports in the literature that need to be considered before reaching such conclusions.[42,45,52,64] Additionally, reports of stable Pd clusters *below the 1.0 nm size*[42,52] offer an alternative hypothesis to, if not suggestive disproof of, CNT for such Pd nanoparticle formation systems. Overall, this report[77] should be read with caution and skepticism towards the conclusions drawn. The experimental set-up remains intriguing so that further studies of this system and by the methods employed would likely be welcomed by the nanoparticle formation community.	77
21	In Situ Time-Resolved XAFS Studies on Laser-Induced Particle Formation of Palladium Metal in an Aqueous/EtOH Solution	Palladium(0) nanoparticles were formed from the reduction of $PdCl_2$ in an aqueous/ethanol solution containing NaCl and polyvinylpyrrolidone (PVP) under N_2. Particle formation was induced using a Nd:YAG laser (266 nm, 10 Hz, 8 ns). The laser fluence was adjusted from 19.9 to 59.7 mJ/cm^2. Kinetics data were collected using DXAFS, and TEM was used to collect	The authors found correlations between the fluence of the UV laser and the resultant particle size. Broadly, they concluded "that laser irradiation with a higher fluence promotes particle growth."[78] The DXAFS-based kinetics data were fit successfully using the FW 2-step mechanism. Analysis of rate constants, extracted from the kinetics data with the FW 2-step mechanism, the k_1' (apparent nucleation rate constant) and k_2' (apparent growth rate constant),	The authors in this study have collected excellent kinetics data using XAFS. The exact, characterization of the palladium(II) in the reaction solution is not known nor is the balanced reaction stoichiometry. Hence, it remains unclear what Pd(II) species is being reduced. The authors were able to fit their data using the FW 2-step mechanism Remaining to be done include: (i) speciation studies on the forms of	78

		particle sizes and size-distributions.	revealed that the fluence of the laser impacted both the nucleation and growth processes.	Pd(II) in solution, such as are Pd^{2+} or $PdCl_xOH_y^{(2-x-y)-}$; (ii) deconvolution of the FW 2-step k_1' (apparent) rate constant (i.e., from their current kinetic treatment of the DXAFS data) into its fuller, underlying nucleation rate law and hence more intimate nucleation mechanism (i.e., as done elsewhere for $Ir(0)_n$ systems discussed in the main text).	
22	Synthesis and formation mechanism of self-assembled 3D flower-like Bi/γ-Fe_2O_3 composite particles	Particles composed of a bismuth core and iron(III) oxide shell were prepared using a hydrothermal process. Metal nitrate salts, potassium hydroxide, ethylene glycol (solvent and reducing agent), and in some cases the surfactant PVP, were used to prepare the particles. Particles were characterized using XAFS, XRD, SEM, HR-TEM, ICP-OES, TGA, DSC, and Raman. No kinetics data was collected, but particles were characterized at 7 points throughout the reaction.	The authors concluded that the Bi/γ-Fe_2O_3 composite was composed "of a Bi metal nucleus and a γ-Fe_2O_3 shell. The Bi metal nucleus is the aggregate of Bi nanoparticles, while the γ-Fe_2O_3 shell results from the intercrossing of γ-Fe_2O_3 nanoslices."[79] These results were determined from analyzing the HR-TEM, XAFS, and XRD data, collected at the 7 different sampling times (0.5, 0.75, 1, 2, 4, 8, and 12 h). In Figure 9 of the paper,[79] the authors report a (cartoon) schematic of their proposed growth mechanism. It consists of hydrothermal treatment of the reaction solutions, nucleation and agglomeration (between 30 min – 1 h), short petal formation (1 h – 2 h), self-assembly and nanopetal growth (2 h – 24 h) and then 3D flower-like composite formation.	The authors have characterized their system at specific points throughout the reaction quite well. Remaining to be done en route to a supported mechanism for this system include: (i) the balanced reaction stoichiometry; (ii) collecting of the necessary kinetics data and overall rate law for particle formation; and (iii) use of a disproof-based[10,10] approach so as to reach more reliable mechanistic conclusions, especially since the present study tends towards a confirmation bias approach.	79
23	Insights into Reaction Intermediates to Predict Synthetic Pathways for Shape-Controlled Metal Nanocrystals	Copper nanoparticles were synthesized from CuBr in oleylamine with either tri-*n*-octylphosphine (TOP) or tri-*n*-octylphosphine oxide (TOPO). A series of hot-injection and heat-up syntheses were conducted to produce Cu	The authors elucidated the speciation of the starting precursors using EXAFS, NMR, and MS. Once the identities of the two precursors were known, the authors monitored the conversion kinetics of the precursors to the Cu(0) nuclei. Then, they used the insights from the conversion kinetics and the	The authors have taken great care to determine the reaction stoichiometry and elucidate the precursor speciation. As mentioned throughout the main text, the reaction stoichiometry and speciation are absolutely essential in order to determine any mechanism of particle formation. This study in	80

		nanoparticles with different morphologies. The syntheses were monitored *in situ* using EXAFS. Further characterization and analysis were done using MALDI-TOF-MS, NMR, TEM, and XRD.	reaction conditions (heat-up vs hot-injection) to manipulate the synthetic environments. The authors were then able to synthesize Cu nanoparticles with different morphologies (cubes, octahedral, truncated octahedral, and tetrahedral. A generalized, qualitative reaction landscape was proposed.	particular is of great interest as the community attempts to not only control particle size and size distribution but particle *shape*. This paper is a must-read as a tutorial for how to elucidate the precursor speciation!	
24	Study of the Chemical Mechanism Involved in the Formation of Tungstite in Benzyl Alcohol by the Advanced QEXAFS Technique	Tungstite nanostructures were synthesized from WCl_6 in benzyl alcohol at 100 °C and studied *in situ* by QEXAFS. Aliquots were extracted from *ex situ* GC measurements. Further characterization was done by XRD.	The authors report on the series of chemical reactions leading to the formation of tungstite nanoparticles. They used GC to quantitatively investigate the organic byproducts produced and determine the speciation. They used XRD on the product throughout the reaction to determine the identity of intermediate species. Finally, they used QEXAFS to *in situ* monitor the different tungsten environments. The authors were able to deconvolute and monitor four species as a function of time: WCl_6 (starting material), WCl_4 (intermediate), $WOCl_4$ (intermediate), and $WO_3 \cdot H_2O$ (product).	This paper was the first in a series of two papers. The other is reported above in Table S2, also as Entry 24. The authors have presented a rigorous study of the reaction solution speciation. They wrote out a series of potential chemical reactions and carefully quantified the byproduct formation in an effort to determine the reaction stoichiometry of their system. Next, they collected kinetics data using QEXAFS and were able to monitor the different species throughout the reaction. Here, they have satisfied the first two requirements of mechanistic study. Next, and of particular interest, would be to derive the kinetics from their proposed reaction steps and then fit their kinetics data. Importantly, the authors do not claim to know the intimate chemical mechanism. This study will be discussed in more detail in the main text, Section 4.3.	81

Table S4. Summary of Papers Using Tandem Techniques: Use of Synchrotron XAFS and/or SAXS in Combination with Another Technique.

Entry	Title	System & Techniques Used to Monitor the Kinetics	Results and Proposed Chemical Mechanism	Conclusions, Insights, and Critical Analysis	Ref.
1	Nanoscopic Pt Colloids in the "Embryonic State"	Platinum colloids were prepared from $Pt(acac)_2$ in toluene under argon at 333 K. Over 4 hours, $Al(CH_3)_3$, also in toluene, was slowly added. The reaction ran for ~24 hours until the solution changed from yellow to black and gas evolution had stopped. Characterization was done ex situ by quenching the aliquot to 195 K with liquid nitrogen. Measurements were taken using NMR (^{1}H, ^{13}C, and coupled to ^{195}Pt), XANES, ASAXS, TEM, and DFT.	The authors present NMR evidence of a $(CH_3)_4Pt$-μ-$(Al(CH_3))_2$-μ-$Pt(CH_3)_4$ "intermediate" complex. However, the exact stoichiometry that is suggested does not equal the NMR results. The XANES measurements and analysis provide evidence of the platinum average oxidation state changing over the first 80 minutes. The EXAFS analysis reveals that the final size particles (~1.2 nm) contain about 53 atoms. The authors claim the formation kinetics, based on their XAFS results, are fit well by a first-order rate equation.	For analysis and comments, see Entry 2 directly below. This 1st entry is the shorter communication, whereas Entry 2 reports the subsequent full paper.	82
2	In Situ Study on the Wet Chemical Synthesis of Nanoscopic Pt Colloids by "Reductive Stabilization"	Platinum colloids were prepared from $Pt(acac)_2$ in toluene under argon at 333 K. Over 4 hours, $Al(CH_3)_3$, also in toluene, was slowly added. The reaction ran for ~24 hours until the solution changed from yellow to black and gas evolution had stopped. Characterization was done ex situ by quenching the aliquot to 195 K with liquid nitrogen. Measurements were taken using NMR (^{1}H, ^{13}C, and coupled to ^{195}Pt), XANES, ASAXS, TEM, and DFT.	The authors present NMR evidence of a $(CH_3)_4Pt$-μ-$(Al(CH_3))_2$-μ-$Pt(CH_3)_4$ "intermediate" complex. They report the exact stoichiometry that is suggested is not equal to the NMR results. Their XANES measurements and analysis provide evidence of the platinum average oxidation state changing over the first 80 minutes. The EXAFS analysis reveals the final size particles (~1.2 nm) contain about 53 atoms. The authors claim the formation kinetics, based on their XAFS results, are fit well by a first-order rate equation.	Overall, the authors have presented valuable evidence for the formation of a Pt-μ-$(Al)_2$-μ-Pt species, but whether this is an on-path or off-path species is not known and will require pre- or post-steady state kinetics to address that challenging mechanistic question. However, before such studies, there are a few points of confusion and concern that need to be addressed. First, the actual versus proposed stoichiometries do not match. Next, there are inconsistencies between results from different techniques, specifically, the DFT calculations do not support the XAFS. More broadly and unfortunately, the study is plagued by attempted *proof*-based and confirmation biased experimentation, where experiments are designed to *prove* rather than to try and	83

				disproof alternative hypotheses. It follows that the conclusions from this work need to be viewed with considerable caution.	
3	Characterization of zinc oxide nanoparticles encapsulated into zeolite-Y: An in-situ combined X-ray diffraction, XAFS, and SAXS study	Zinc oxide particles prepared inside zeolite Y were prepared by ion-exchange between sodium zeolite Y (Si/Al – 2.52) and aqueous zinc acetate at room temperature for 24 hours. Then, the zinc zeolite Y was treated with sodium hydroxide "to precipitate the oxide nano-particles inside the zeolite framework."[84] The authors performed both XAFS-XRD and SAXS-WAXS on the system by calcinating the particles from 25 ºC to 550 ºC and 25 ºC to 300 ºC, respectively, at a rate of 5 ºC/min.	Based on XRD, the authors found no large zinc oxide particles. By XAFS, the authors found "only minor changes take place during the heat treatment process", and they "estimated the particle size by calculating the variation in coordination number of Zn–Zn for different cluster sizes…and we obtained a value of ~18 ± 4 Å."[84] Finally, the authors report a particle size of ~15 ± 5 Å by SAXS. Both the EXAFS and SAXS values are consistent with the size of the zeolite Y cage.	The authors have demonstrated the usefulness of the various synchrotron techniques, namely tandem XAFS-XRD and SAXS-WAXS. Importantly, they have not attempted to make conclusions beyond the scope of their data and the techniques used. They claim to have characterized the material. Then, they characterize it and state further inferences will require additional study. Careful, thoughtful, proper science and conclusions, in our opinion.	84
4	Structure of assemblies of metal nanowires in mesoporous alumina membranes studied by EXAFS, XANES, X-ray diffraction and SAXS	The authors studied four different metal nanowires formed inside anodic aluminum oxide (AAO) membranes. The AAO membranes were prepared by anodizing aluminum foils in polyprotic acid using a lead plate cathode. The pore diameters were controlled by the anodizing voltage. The resulting pores used were 12, 24, 48, and 72 nm. Nanowires of iron, cobalt, tin, and gallium nitride were prepared. Iron, cobalt, and tin were prepared "by electrochemical AC plating from an aqueous solution of metal sulfate, with H_3BO_3 as a supporting electrolyte in the case of iron and cobalt, and H_2SO_4 in the case of tin."[85] Gallium nitride nanowires were prepared from thermally decomposing $Ga(NO_3)_3$ at 1000 °C to	The iron nanowires were found to retain the same structure as bulk iron. However, the electronic structure of the iron nanowires appears to be correlated to the size of the AAO pore diameter. The cobalt nanowires appear to form a convolution of hcp and fcc structures depending on the nanowire diameter. The exact dependence was unable to be elucidated, as it was found that the ratio of the two structure types (hcp:fcc) was not linear with nanowire diameter. The tin nanowires were found to "become superconducting at the same temperature as bulk tin: 3.7 K."[85] The GaN nanowires were found to have a hexagonal wurtzite structure. However, extra heating in the synthesis process to 1150 °C resulted in incorporation of some aluminum into the structure.	Of note, the authors state in their conclusion that their "philosophy is that detailed characterization of the structures of assemblies of metal and semiconductor nanowires within AAO membranes is an essential prerequisite to understanding and controlling their physical properties."[85] *Noteworthy is that this philosophy is the proper foundation from which to conduct mechanistic research by any scientist.* One must fully characterize a material before being able to design meaningful kinetics and mechanistic experiments. Why, one might ask? Because the proposed steps of the mechanism must add up to the observed, balanced reaction—otherwise, one is proposing a mechanism for some other reaction than the one at hand. Often, even trace	85

		gallium oxide, and then reacting that with NH_3 at 1000 °C. Nanowires were studied using EXAFS, XANES, WAXS, HE-XRD, and SAXS.		products or by-products can provide detailed insight into the underlying mechanism. A good example is trace R-R, R-H and R(-H) (olefin) products: these are often definitive indicators of R• intermediates, each R• giving characteristic R-R, R-H and R(-H) that vary little from the gas phase to different solvents.	
5	A Combined SAXS/WAXS/XAFS Setup Capable of Observing Concurrent Changes Across the Nano-to-Micrometer Size Range in Inorganic Solid Crystallization Processes	The authors have presented a unique multi-technique (SAXS/WAXS/XAFS) set-up to study the crystallization process of an inorganic-aluminum phosphate solid. The authors have identified the stoichiometry as $Zn_xAl_{1-x}PO_4$, prepared from the combination of zinc nitrate hydrate, H_3PO_4, triethylamine, and pseudoboehmite alumina.	The extent of crystallization was determined as a function of the increase in temperature. Initial WAXS peaks were observed after the temperature reached 90 °C, and the peaks increased until 160 °C. At that point (160 °C), the reaction was determined to have reached completion. The final crystallite size was calculated (by Scherrer analysis) to be ~54 nm. Based on the SAXS/WAXS/XAFS results, the authors proposed "that growth occurred via a two-step aggregation/crystallization process."[86]	This paper demonstrates the power of combining several direct techniques. As the authors say, for many studies of crystallizations, workers "often focus on data acquired using a single technique, which rarely provides all of the necessary information from which new insight can be obtained."[86] Here, the authors have shown the crystallization and broader scientific communities that effectiveness of using tandem, direct techniques. Needed in the following case to upgrade the proposed two-step growth process to a more reliable mechanism include: (i) knowledge of the complete, balanced reaction stoichiometry; (ii) postulation of pseudo-elementary reaction steps for all possible reasonable alternative mechanisms; and (iii) testing those mechanisms by attempted fittings of the kinetics data, all with a disproof of alternative mechanistic hypotheses as the *modus operandi.*	86
6	XAFS, SAXS, and HREM characterization of Pd nanoparticles	Palladium nanoparticles, capped by thiols, were prepared by combining $PdCl_2$ with *n*-alkyl thiol (*n* = 12, 16, or 18; hereafter, SC12, SC16, and	The resulting nanoparticles were observed, by HR-TEM and SAXS, to have "diameters of 1.2 ± 0.4 nm, 1.2 ± 0.4 nm and 1.3 ± 0.5 nm for Pd:SC12,	This paper presents an excellent summary of the characterization for these tiny palladium nanoparticles. These contain the necessary experiments	87

	capped with *n*-alkyl thiol molecules	SC18), and lithium triethylborohydride in THF. The reaction was run at 60 °C for 16 hours before purification in cold ethanol and toluene. Characterization was performed using HR-TEM, XAFS, and SAXS.	Pd:SC16 and Pd:SC18, respectively."[87] The particles from the Pd:SC12 synthesis were found to retain a metallic Pd core, while the particles from the Pd:SC18 synthesis were found to have converted completely to a PdS structure. Restated, as the authors state, "[t]he volume sulfidation in total in nanoclusters capped with thiol with long carbon chains (n = 18) and only partial in nanoclusters with short carbon chains (n = 12), the core of the particles remaining in this case in metallic state."[87]	to understand the final product stoichiometry. While no mechanistic or kinetics data are collected, the techniques used (SAXS and XAFS) could easily be applied to monitor the formation process of the palladium nanoparticles.	
7	*In situ* observation of formation of silver particles in water-in-scCO_2 emulsions	Silver nanoparticles were prepared by two methods: photoreduction by UV light and chemical reduction by hydrazine. Reaction solutions were made of silver perchlorate, AOT (di-2-ethylhexyl sodium sulfosuccinate), benzoin, small amount of F-pentanol (2,2,3,3,4,4,5,5-octafluoro-1-pentanol), ethanol, water, and CO_2. The experimental cell was kept at 35 ºC and 25 MPa for 5 hours with stirring to form the homogeneous emulsions prior to either irradiation with UV light or addition of hydrazine. The reaction was monitored by either EXAFS or tandem UV-vis and SAXS.	The authors found, by both TEM and SAXS, that the average diameter or the Ag particles "prepared by the photoreduction and by the hydrazine reduction in the microemulsions is estimated…to be 6.4 and 2.9 nn, respectively."[88] The analysis of the size distribution reveals a rather large error in average diameter, ca. 28-62%. However, the SAXS analysis revealed that the size of the water droplets has a negligible effect on the Ag particle formation. Furthermore, the authors found the EXAFS "demonstrate that Ag^+ ions were completely reduced to Ag^0 atoms and the formation of Ag-Ag bond occurred in the AOT-rich phase by the hydrazine reduction, followed by the subsequent formation of larger Ag particles, while these Ag^+ ions were not completely reduced in the photoreduction of the concentrated Ag colloidal dispersions."[88]	This study demonstrates how careful, *tandem* experimentation is quite powerful. The combination of two direct techniques (SAXS and UV-vis) to monitor the size and electronic evolutions can provide the necessary, rigorous kinetics from which to conduct mechanistic investigations. This study is a good foundation upon which to begin a mechanistic study. The needed additional studies en route to a disproof-based minimum mechanism include: (i) determination of the balanced stoichiometry; (ii) writing out the entire list of pseudo-elementary step based plausible mechanisms; (iii) fitting the data to those mechanisms—and where fits are not possible, thereby (iv) disproof of alternative mechanisms for the formation of silver nanoparticles in water-in-scCO_2 emulsions. What would likely be of fundamental interest is (v) determining, from control experiments leaving out components such as the	88

				$scCO_2$ if / where possible, what the roles of those components are in the Ag_n particle formation process.	
8	Influence of Monomer Feeding on a Fast Gold Nanoparticles Synthesis: Time-Resolved XANES and SAXS Experiments	Gold nanoparticles were synthesized in toluene from $AuCl_3$ (7 mM) The ligand was either decanoic acid or decylamine. Didodecyldimethylammonium bromide (DDAB) was used as a cationic surfactant. Tetrabutylammonium borohydride (TBAB) was used as a reductant. Ligand was added in a 14:1 ratio to Au starting material. DDAB:Au and TBAB:Au were both 4:1. The authors performed kinetics experiments using XANES and separate kinetics experiments using SAXS.	The authors claim to have "assessed in situ and quantitatively the fast formation process of gold nanoparticles in solution."[89] "An important result of these experiments is that during the reduction of Au(I) a measurable amount of Au(0) appears in bulk which shows that the model of a supersaturation of bulk monomer can be used."[89] Further, when the authors studied the effect of the ligand, they found "that the stabilizing ligand controls the size of the nanoparticles by controlling the formation rate of monomers. However, the molecular mechanism at play which could yield these differences remains difficult to assess rigorously."[89] The authors also used CNT to fit their data and the "Lamer scheme"[89] to explain their concentration of Au(0) monomer versus time plot.	The authors have presented an intriguing study for the formation of Au nanoparticles. They have expertly chosen to study directly the particle formation using XANES (for the Au oxidation state) and SAXS (for the particle size and size distribution), both as a function of time. However, it should be noted that the SAXS and XANES measurements were taken at different times and different locations, so while they are under the same conditions, they were separate experiments. The authors claim that CNT can be used for their system, yet there is presently no evidence in the literature for CNT being able to successfully explain metal particle formation.[13] The authors cite "a burst of the number of particles is in direct agreement with the old Lamer scheme"[89], which is a claim that has been disproven in two recent reviews.[12,13] Finally, the authors claim that "three processes occur concomitantly: formation of new monomers through reduction of the precursors (either in bulk or at the surface), nucleation of new particles, and growth of the existing particles."[89] The authors miss that *if* reduction of metal, nucleation of kinetically effective nuclei, and growth are all taking place at the same time as they claim, *then* CNT and the LaMer model are disproven by the author's own data Overall, this study	89

				illustrates an excellent choice of instrumentations and the collection of excellent data, but the interpretation of the data needs further examination.	
9	Mechanism of Gold Nanoparticle Formation in the Classical Citrate Synthesis Method Derived from Coupled In Situ XANES and SAXS Evaluation	Gold nanoparticles were prepared according to the original procedure by Turkevich,[90] where an aqueous solution of $HAuCl_4$ and $Na_3Citrate$ were mixed at 75 ºC. Measurements were taken in situ by tandem SAXS/XANES using an acoustic levitator as the sample holder. Further characterization was done by UV-vis, SEM, and TEM.	The authors report high-quality tandem SAXS/XANES studies leading to time-resolved size, number of particles, polydispersity, and oxidation state data. From these data the authors propose a 4-step gold nanoparticle formation pathway consisting of the words of "fast initial formation of small nuclei, coalescence of the nuclei into bigger particles, slow growth of particles sustained by ongoing reduction of gold precursor, and subsequent fast reduction ending with the complete consumption of the precursor species."[91]	While the data presented is impressive, there are numerous points of discussion to some concerns with the analysis. First, one should realize that the data are not all collected in situ, but "at different reaction time, ca. 4 μL of the liquid samples were extracted from the catch of reaction solution and placed as droplets in an acoustic levitator".[91] Second, the authors did not quantitatively, nor even qualitatively, fit their high-quality kinetics data to any mechanism. They claim to have determined a 4-step "mechanism", but in fact have not done any of the necessary steps to get to such mechanism that goes beyond just words. Notably, the needed studies are: (i) determination of the balanced reaction stoichiometry; (ii) writing out pseudo-elementary steps for all reasonable mechanisms along with their associated differential equations, (iii) then attempted fitting the kinetics data to each mechanism, all with (iv) a disproof-and Ockham's razor approach as the history of chemical mechanisms from physical-organic chemistry teaches is required to reach a reliable mechanism. Furthermore, the authors have described "the initial step as burst nucleation"[91], which is a concept from the LaMer model that has been definitively disproven,[12,13] a critical insight that future studies need to take into account.	91

10	In Situ and Simultaneous UV—vis/SAXS and UV—vis/XAFS Time-Resolved Monitoring of ZnO Quantum Dots Formation and Growth	Zinc oxide quantum dots were prepared from the zinc tetramer, Zn_4OAc_6, in absolute ethanol at 40 ºC. The hydrolysis and condensation reactions were catalyzed by the addition of KOH. In situ tandem measurements were taken using UV-vis/XAFS and UV-vis/SAXS.	Based on time-resolved data, the authors proposed a four-step schematic for the temporal evolution of the zinc oxide quantum dots. The authors claim the formation of the ZnO quantum dots "is a step process composed of four main stages: (i) ZnO Qdot nucleation and growth; (ii) growth of compact ZnO Qdot aggregates; (iii) growth of fractal aggregates; and (iv) secondary nucleation and fractal aggregates growth."[92] The exact nucleation process was not able to be elucidated "due to the experimental time acquisition", as "too little information was collected in that period of time to be able to give a quantitative analysis of this initial nucleation process."[92]	The authors in this paper have expertly collected tandem, direct, time-resolved particle size data. As noted, they have recognized when they were unable to collect quantitative data and wisely have not attempted to make conclusions beyond their data. Unfortunately, the authors have relied only on equations from models that do not fit their data. Needed before a reliable mechanism can be obtained are once again just those exact steps and approach listed in entries 5, 7, and 9 in this Table S4.	92
11	Probing Nucleation Pathways for Morphological Manipulation of Platinum Nanocrystals	Platinum nanocrystals were synthesized from two reaction solutions. Both systems used tetrachloroplatinate(II) and the stabilizer PVP. The first system used ethylene glycol (EG) as the solvent and reducing agent. The second system used citric acid (CA) as the reducing agent and water as the solvent. Nanocrystal formation was monitored by tandem in situ QXAFS and UV-Vis. Specifically, the EXAFS were analyzed.	The authors report that the EG synthesis produced nanocrystals with a nanowire morphology. Meanwhile, the CA synthesis produced nanospheres. The XAFS and UV-Vis results support the morphologies observed by TEM. The authors postulate that EG is a "weak" reductant, compared to CA, and does not completely reduce the Pt(II). This produces $[Cl_3Pt—PtCl_3]^{4-}$ dimers that polymerize into "longer line 'Pt_nCl_x' complexes."[93] CA is believed to immediately reduce Pt(II) to Pt(0). Hence, a cartoon mechanism is proposed for each reductant. For EG, $[PtCl_4]^{2-}$ is partially reduced to form $[Cl_3Pt—PtCl_3]^{4-}$ dimers, then longer "dimer clusters", and finally, a "linear Pt_nCl_x complex".[93] For CA, $[PtCl_4]^{2-}$ is	The concept of "reducing strength" is intriguing, but qualitative and hence impossible to test quantitatively. Numerous scientific questions arise from this work that additional studies will hopefully address: (i) what is the effect of having EG versus water as the solvent;? (ii) what direct evidence is there for the formation of $Pt(0)_{2-3}$ clusters?; (iii) what is the speciation of the reaction solution?; and (iv) what differential equations were used to fit the kinetics data that produced the (cartoon) mechanism shown in Figure 4 within of that paper?.[93] Overall, the authors have collected impressive, high-quality synchrotron data, but gaps in needed evidence and a lack of mechanistic analysis are issues	93

			reduced to Pt(0) atoms, the $Pt(0)_2$ and $Pt(0)_3$ clusters, and finally "spherical $Pt(0)_n$ cluster".[93]	that merit attention.	
12	Understanding Solvothermal Crystallization of Mesoporous Anatase Beads by In Situ Synchrotron PXRD and SAXS	The crystallization of TiO_2 beads was performed using three different amorphous precursor beads (between 0.3 – 1.1 microns), titanium(IV) isopropoxide (TIP), hexadecylamine (HDA), potassium chloride, ammonia, and water. The reaction was monitored using in situ synchrotron PXRD and SAXS. Ex situ measurements were conducted using SEM, TEM, and SAED.	The authors conclude the crystallization from the amorphous TiO_2 beads "to be a 3-dimensional crystallization process involving 4-steps. This process involves (1) an induction period for HAD (organic structure-directing agent) and amorphous TIO_2 dissolution, (2) anatase nucleation and growth at the expense of precursor dissolution, (3) coarsening in anatase crystals accompanied by continued precursor dissolution, and (4) reaching stable crystallite size with no significant Ostwald ripening."[94]	The authors have collected excellent data using the best techniques available, directly and in situ. They have attempted to provide alternative hypotheses throughout their study. The authors have constructed a "words-only" 4-step mechanism based on their qualitative results—so that an issue is that no significant quantitative results are given to support their claimed 'mechanism'. This study, too, needs the stepwise, disproof-based mechanistic approach outlined in entries 5, 7, 9 and 10 directly above in this Table S4.	94
13	Mechanisms of SnO_2 Nanoparticles Formation and Growth in Acid Ethanol Solution Derived from SAXS and Combined Raman–XAS Time-Resolved Studies	SnO_2 nanoparticles were prepared from $SnCl_4 \bullet 5H_2O$ in absolute ethanol at pH = 0.9. Water was added slowly over 9 minutes, and the solution was aged for 30 minutes at room temperature. Next, the solution was heated from 30 ºC to 70 ºC at a rate of 1 ºC/minute. Once the solution reached 70 ºC, it was aged a further 60 minutes. The reaction was monitored in situ by tandem QXAFS and Raman, and a separate in situ SAXS experiment. In addition, ex situ measurements were taken using XRD and HR-TEM.	The authors have thoroughly investigated the speciation of the water-ethanol-tin solution that occurs at room temperature. They have identified the three primary components as $[SnCl_x(H_2O)_{6-x}]^{4-x}$, where x = 3, 4, or 5. Next, the authors have presented numerous figures of XAFS or SAXS output versus time. Based on their results, the authors proposed "a five-step mechanism of formation"[95] for their system. "The first three steps…correspond to the prenucleation of low nuclearity species, followed by a monomer – tin oxo cluster aggregation growth and cluster-cluster growth, leading to the formation of double or triple chains structure further interconnected for form SnO_2 nanoparticles."[95] During the heating and	Overall, the authors have collected superb data on a fascinating system. Their thorough investigation into the solution speciation before nanoparticle formation is noteworthy and commendable. The issues with this work are: they claim a mechanism without having written out the integrated rate law. In their[95] Figure 3, they have fit the "two linear growth regimes…with two distinct kinetic rates k" from the rate function "$Rg - Rg_0 = kt$", which they claim "indicate behaviour consistent with the reaction-limited growth kinetics controlled by two different mechanisms."[95] Yet, they have not further investigated these claimed mechanisms. At the end of the paper, the authors claim "these five well time-defined stages can be used as a	95

			aging at 70 ºC, “a densification process followed by an advanced nanocrystallite growth through the addition of mononuclear species to the surface of the nanoparticles has been identified.”[95]	versatile way to control the growth processes in order to fine tune the size of SnO_2 nanocrystalline particles.” This claim is not demonstrated or substantiated anywhere in their paper nor by any literature they have cited. Overall, this study has collected first-rate synchrotron data and performed noteworthy, due diligence on the solution speciation. That said, they do not have a mechanism by the established criteria of obtaining a reliable reaction mechanism.	
14	Synthesis of 1nm Pd nanoparticles: Insights on the synthesis mechanism using *in situ* XAFS and SAXS in a microfluidic reactor	Palladium nanoparticles were synthesized from palladium acetate in a 1:1 mixture of toluene and alcohol, in the presence of either oleylamine (OLA) or trioctylphosphine (TOP). The OLA-stabilized particles were synthesized at 60 ºC in a toluene/methanol solution at an OLA:Pd molar ratio of 1:1. The TOP-stabilized particles were synthesized at 100 ºC in a toluene/hexanol solution at a TOP:Pd molar ratio of 1.5:1. Particle formation was done inside a microfluidic reactor and monitored by tandem in situ SAXS and XAFS. STEM measurements were done ex situ.	The authors found for both OLA and TOP that “nucleation proceeded continuously over the time period analyzed and was overlapped by an autocatalytic growth phase without causing a broad size distribution.”[96] Furthermore, and despite there still being a significant amount of unreacted precursor in solution, “the growth rate was observed to slow considerably and the nanoparticles size reached a plateau with a narrow size distribution.”[96] “The combined SAXS and XAFS results strongly suggest the ligands play an important role in affecting the nucleation and growth rates leading to the self-limiting nanoparticle size observed.”[96]	The authors have presented an intriguing study of TOP- and OLA-stabilized Pd nanoparticles. Importantly, and as they state it, the “coupling of multiple in situ techniques is needed to provide a more detailed, near complete picture of the synthesis mechanisms.”[96] The use of synchrotron-based X-ray scattering and spectroscopy techniques are of particular interest to obtain size, shape, chemical, and structural information. Of particular note, the authors have not attempted to draw conclusions beyond what the data has presented. The author has presented the available particle formation mechanisms in the literature and systematically ruled out each of them. The one that most closely matches their data is the FW 2-step mechanism, and significant is that the authors further illustrate how it is not entirely effective / limited for the case at hand because ligand effects—which are shown to significantly contribute to this system—go beyond the minimum FW 2-step	96

				mechanism. Overall, this paper is an important study headed in the proper direction, one that *does not* attempt to draw conclusions beyond what the data has shown. Items for future study include: (i) a complete reaction stoichiometry, (ii) kinetics derivation, and fitting of kinetics data to plausible mechanisms explicitly containing ligand effects.	
15	Simultaneous SAXS/WAXS/UV-Vis Study of the Nucleation and Growth of Nanoparticles – A Test of Classical Nucleation Theory	Gold nanoparticles were prepared from $AuPPh_3Cl$ in toluene with dodecanethiol (DDT) and *t*-butylamine borane (TBAB), sonicated together at room temperature. The Au solution was combined with the TBAB (also in toluene) using a stopped flow device for measurements by in situ, tandem SAXS, WAXS, and UV-vis. TEM was used to characterize the resultant Au nanoparticles.	The authors used their in situ SAXS/WAXS/UV-vis technique to "study the kinetics as a function of the most relevant parameters such as concentration, temperature, ligand ratio, and the addition of polar cosolvents."[97] The authors claim to have, for the first time, "numerically solved the complete set of reaction rate equations comprising precursor reaction, nucleation, growth, and Ostwald ripening to obtain the evolution of the full particle size distribution from the induction period to the late growth stage."[97] Finally, the authors have presented a schematic presentation of Au nanoparticles growth based on their results and the components they believe are involved in the formation mechanism.	Noteworthy are the authors' unique tandem in situ technique and excellent resultant data! Next, the authors claim their model fits their data well; however, in their Figure 2a, the model fails to fit the early time data. It may be that their growth model fits the growth-dominated portion of the kinetics data, but the majority of the nucleation data is missed. The authors report a "fast nucleation (LaMer mechanism)"[97], but the LaMer mechanism at least, especially at room temperature, has been thoroughly disproven.[12,13] Overall, the authors experimental approach is impressive, and the fitting of the growth data is well performed. Requiring attention are the overlooked assumptions used in the nucleation model that cause the model to not work for this system. Further investigations along the lines discussed for entries 5, 7, 9, 10, 12, and 14 are needed before a more complete, reliable mechanism for this particular Au nanoparticles system can be claimed to be in hand.	97
16	*In situ* studies on	Polydisperse gold nanoparticles were	The authors monitored the reaction over	The authors present an intriguing study	98

	controlling an atomically accurate formation process of gold nanoclusters	prepared by reduction of $Au_2(L_3)_2Cl_2$, where L_3 = 1,3-bis(diphenylphosphino)propane, with $NaBH_4$ in dichloromethane. The polydisperse Au_n clusters were re-dispersed in ethanol, where HCl was added to initiate the formation of monodisperse $Au_{13}(L_3)_4Cl_4$ clusters. The "size-convergence" "etching" process was monitored by tandem, in situ UV-vis and XAFS. Ex situ measurements were taken using MALDI-MS.[98]	a 10-hour period, where they observed Au_n (n ~ 15–65) "size-converge" to Au_{13} clusters.[98] Within hour 1, new peaks appeared in the UV-vis spectrum indicating particles of Au_8–Au_{13} (primarily Au_{11}), corroborated by MALDI-MS. By hour 2, particles of size Au_{30}–Au_{40} had disappeared, and absorption data suggested the formation of Au_{13}. Overall, the authors "found that the cluster formation is achieved in an etching/growth manner including two distinct reaction steps. (1) The initial polydisperse Au_n clusters are etched by HCl."[98] And (2) "a secondary-growth step to form uniform $Au_{13}(L_3)_4Cl_4$ clusters, by incorporating the reactive Au(I)–Cl species in the solution."[98]	of the secondary growth/etching in polydisperse Au_n nanoparticles treated with HCl. They have collected solid XAFS, MS, and UV-vis data. Remaining for future study are a better mechanistic understanding for "the etching mechanism during nanocluster formation".[98] Primarily, the authors use MS and their "schematic illustration" to attempt the impossibility of "deducing" the correct mechanism—that is, vs the proper approach of offering solutions for the inverse problem where on gets to "cause" (here, the mechanism) from "effects / observables" by inductively disproving ones way there. Hence, in order to claim they have the "etching mechanism", the steps noted already for entries in this Table S4 (Entries 5, 7, 9, 10, 12, 14, and 15) will be required.	
17	Time-resolved *in situ* studies on the formation mechanism of iron oxide nanoparticles using combined fast-XANES and SAXS	Iron Oxide nanoparticles were prepared from an equal mixture of $FeCl_3$•$6H_2O$ and $FeCl_2$•$4H_2O$ in water (total Fe concentration of 0.31 M) and mixed with triethanolamine (TREA). The reaction was run for 1.5 h at 115°C. The reaction was monitored using tandem XANES and SAXS with an acoustic levitator as a sample holder. Ex situ TEM and XRD were used to characterize the resultant iron oxide nanoparticles.	The authors collected time-resolved XANES and SAXS results, as well as characterized the "first intermediate species"[99]. Then, they characterized the final product using TEM and XRD. Based on their experimental results, the authors claim a formation mechanism consisting of four phases. Paraphrasing, the four phases are: (i) formation of akageneite as an intermediate Fe_xO_y species; (ii) formation of magnetite particles (~3 nm); (iii) growth of magnetite nanoparticles; and (iv) maghemite nanoparticles grow to "a radius of gyration of 4.2 nm".[99]	The authors have examined the case of FeO_x nanoparticle formation using a creative tandem XANES and SAXS set-up. The complete, balanced reaction stoichiometry has not been presented. Kinetics data have been monitored. However, the kinetics data is not in a form, yet, that can be fit by an analytic equation. No pseudo-elementary steps or corresponding differential equations have been written for the proposed mechanism. Finally, the authors have started the needed disproof-based experimentation with their assessment over HCl's role in the reaction; the disproof of additional plausible mechanisms would be most welcome. Overall, this system and its creative	99

				experimental set-up, warrants further use to elucidate a complete mechanism for FeO_x formation.	
18	Concerted Growth and Ordering of Cobalt Nanorod Arrays as Revealed by Tandem in Situ SAXS-XAS Studies	Cobalt nanoparticles were synthesized from $[Co\{N(SiMe_3)_2\}_2(THF)]$, lauric acid (LA), and hexadecylamine (HDA) at 130 or 150 ºC and reduced under ~50 psi H_2. Particles were analyzed ex situ by TEM and SEM. Tandem XAS and SAXS experiments collected kinetics data on the formation of the nanorods.	Based on the authors tandem XAS-SAXS experiments, in conjunction with their ex situ TEM images, the authors propose "a qualitative nanorod growth mechanism, which consists of three main steps: a fast nucleation, a fast growth by monomer addition that takes place during reduction of Co(II) species to Co(0), and a slower ripening step that takes place after complete reduction, which most likely involves an oriented attachment process."[100] In addition, the authors have proposed a reaction pathway for the overall nanorod formation.	The authors have produced excellent *qualitative* evidence and analysis for their proposed reaction pathway (presented as Scheme 1 in the paper[100]). Of note, their use of tandem XAFS and SAXS displays the power of tandem, in situ techniques for monitoring particle formation and developing mechanistic insights. Further, they applied disproof (or at least consideration) of alternative hypotheses to their results. The only drawback, as the authors note, is that they were not able to collect particle volume (number) data with their current set-up. Hence, they were only able to collect *qualitative* data. With additional *quantitative* data, they may be able to determine what the mechanism of nucleation and/or growth is for cobalt nanorod arrays. Currently, they have proposed fast nucleation and fast growth by monomer addition, which based on their present data could also be interpreted as continuous nucleation and autocatalytic surface growth according to the FW 2-step mechanism. Overall, the authors have produced an excellent, intriguing piece of research that deserves further study and, then, more detailed mechanistic analysis and interpretation.	100
19	Nucleation and Growth Kinetics of ZnO Nanoparticles Studied by in Situ Microfluidic	ZnO nanoparticles were prepared by mixing solutions of zinc oleate in THF and tetrabutylammonium hydroxide (1 M in methanol) in THF. A stopped-flow microfluidic capillary	The authors reported particle size (radius) as a function of time for the four experimental conditions. Data were collected across the first 1000 s of the reaction. A set of differential	The authors have presented a fascinating study of ZnO formation, examined via a creative and effective *in situ* microfluidic set-up. However, they were unable to determine the exact reaction	101

	SAXS/WAXS/UV–Vis Experiments	was used. The reaction was monitored *in situ* using a SAXS/WAXS/UV-Vis set-up with a copper heating tube integrated into the *in situ* capillary holder. Kinetics experiments were conducted at two zinc concentrations (160 and 53 mM) and two temperatures (40 and 50 °C).	equations were written based on the net reaction of Zn^{2+} and 2 OH^-. Then, Classical Nucleation Theory (CNT) was applied to describe the nucleation process and incorporated into the final differential equations. The authors claim that their model was able to fit ca. 50% of the radius versus time data.	stoichiometry. Excellent kinetics data were collected using state-of-the-art synchrotron methods, but the differential equations that were written are based on a single, net ion chemical reaction combined with CNT rather than writing out a full set of pseudo-elementary step reactions. Hence, the set of studies discussed in Entries 5, 7, 9, 10, 12, 14 and 15 in this Table S4 are recommended for emphasis with this ZnO nanoparticle formation system.	
20	The role of pre-nucleation clusters in the crystallization of gold nanoparticles	Gold nanoparticles or gold nanowires were synthesized from 20 mM $AuCl_4^-$, 1 M triisoprpylsilane (TIPS), and 50-400 mM oleylamine (OY) in hexane. The reaction was monitored *in situ* by SAXS, XAS, and HE-XRD (for PDF analysis). Ex situ TEM images were collected	First, the authors determined the balanced stoichiometry for the reduction reaction. Then, they monitored both particle size and gold oxidation species as a function of time. They observed that at high OY concentrations, nanowires formed, whereas at low OY concentrations, ordered nanoparticles formed. Finally, the authors report a series of differential equations that were used to fit the two kinetics datasets based on hypothesized kinetic models for nanowire or nanoparticle formation.	The authors have presented a compelling case for their proposed kinetic models. First, they have written out the balanced chemical reaction and determined the reaction speciation as best they could. Next, they have collected state-of-the-art kinetics data by multiple physical methods. Then, they hypothesized a kinetic model and wrote the differential equations. *Excellent!* These were then solved using numerical integration in MatLab, and they were shown to *fit the kinetics curves*. Finally, an attempt was made to consider at least one additional kinetic model from the literature[7]. Furthermore, the concept of a prenucleation cluster was introduced, although the exact speciation was unable to be determined. The authors note that future studies are needed, a correct statement that in no way diminishes the value of this first-rate study, its mechanistic insights, all of which are a great, recommended read, in our opinion!	102
21	Structural Changes	The formation of a bismuth oxide	The authors report the PDF results of	The authors have demonstrated the	104

	during the Growth of Atomically Precise Metal Oxido Nanoclusters from Combined Pair Distribution Function and Small-Angle X-ray Scattering Analysis	nanocluster, with a $[Bi_{38}O_{45}]$ core from the starting nanocluster $[Bi_6O_5(OH)_3(NO_3)_5]\bullet 3H_2O$ in DMSO, was analyzed using *in situ* Pair Distribution Function (PDF) and SAXS. Further, the authors developed "an automated modelling approach[103] to identify intermediates and the reaction pathway."[104]	the Bi_xO_y structure throughout the reaction. They corroborate these results with SAXS and DLS. These data demonstrate a transformation from the $[Bi_6O_8]$ starting unit cell, to the intermediate $[Bi_{22}O_{26}]$, and to the final $[Bi_{38}O_{45}]$ cluster. The authors report a fast transition from $[Bi_6O_8]$ to $[Bi_{22}O_{26}]$, where it was not possible to identify any intermediate species. The authors report their proposed reaction pathway and recommend their method for other metal oxo cluster systems.	power and effectiveness of combining SAXS with PDF studies. Incorporating an automated modelling approach allowed the authors to deepen their understanding of the PDF results and identify the $[Bi_{22}O_{26}]$ intermediate. Therein, they carefully do not claim to know the complete reaction mechanism, but have faithfully reported the observed, atomically precise structural changes during the growth process. Two important quotations from the paper are: (i) "SAXS and PDF studies may allow the identification of prenucleation clusters, and provide a much deeper understanding of the fundamental processes involved in nucleation"[104] and (ii) "understanding the solution chemistry of metal oxido clusters on an atomic and molecular scale can thus open new opportunities for synthesizing nanoscale metal oxides in a controlled manner."[104] These quotes represent the power and potential of using PDF in combination with another in situ synchrotron technique. We highly recommend this paper for others investigating crystalline systems!

REFERENCES

[1] Avrami, M. Kinetics of Phase Change. I. General Theory. *J. Chem. Phys.* **1939**, *7*, 1103-1112.
[2] Avrami, M. Kinetics of Phase Change. II. Transformation-Time Relations for Random Distribution of Nuclei. *J. Chem. Phys.* **1940**, *8*, 212-224.
[3] Avrami, M. Kinetics of Phase Change. III. Granulation, Phase Change, and Microstructure. *J. Chem. Phys*. **1941**, *9*, 177-184.
[4] Gibbs, J. W. On the Equilibrium of Heterogeneous Substances. *New Haven Transactions of Connecticut Academy of Arts and Sciences* **1874**, *III*, 343-523.
[5] Volmer, M. *Kinetik der Phasenbildung*. Verlag von Theordor Steinkopff: Leipzig, 1939.
[6] Becker, R.; Döring, W. Kinetische Behandlung der Keimbildung in übersättigten Dampfen. *Ann. Phys.* **1935**, *24*, 719-752.
[7] Watzky, M. A.; Finke, R. G. Transition Metal Nanocluster Formation Kinetic and Mechanistic Studies. A New Mechanism When Hydrogen Is the Reductant: Slow, Continuous Nucleation and Fast Autocatalytic Surface Growth. *J. Am. Chem. Soc.* **1997**, *119*, 10382-10400.
[8] Liftshitz; I. M.; Slyozov, V. V. The kinetics of precipitation from supersaturated solid solutions. *J. Phys. Chem. Solids* **1961**, *19*, 35-50.
[9] Wagner, C. Z. Theorie der Alterung von Niederschlägen durch Umlösen. *Electrochem.* **1961**, *65*, 581-591.
[10] Platt, J. R. Strong Inference. *Science* **1964**, *146*, 347-353.
[11] Chamberlain, T. C. Studies for Students. The Method of Multiple Working Hypotheses. *J. Geology* **1897**, *5*, 837-848.
[12] Whitehead, C. B.; Özkar, S.; Finke, R. G. LaMer's 1950 Model for Particle Formation of Instantaneous Nucleation and Diffusion-Controlled Growth: A Historical Look at the Model's Origins, Assumptions, Equations, and Underlying Sulfur Sol Formation Kinetics Data. *Chem. Mater.* **2019**, *31*, 7116-7132.
[13] Whitehead, C. B.; Özkar, S.; Finke, R. G. LaMer's 1950 Model of Particle Formation: A Review and Critical Analysis of Its Classical Nucleation and Fluctuation Theory Basis, of Competing Models and Mechanisms for Phase-Changes and Particle Formation, and then of Its Application to Silver Halide, Semiconductor, Metal, and Metal-Oxide Nanoparticles. *Mater. Adv.* **2021**, *2*, 186-235.
[14] Whitehead, C. B.; Watzky, M. A.; Finke, R. G. "Burst Nucleation" vs Autocatalytic, "Burst" Growth In Near-Monodisperse Particle Formation Reactions. *J. Phys. Chem. C* **2020**, *32*, 3657-3672.
[15] LaMer, V. K.; Dinegar, R. H. Theory, Production and Mechanism of Formation of Monodispersed Hydrosols. *J. Am. Chem. Soc.* **1950**, *72*, 4847-4854.
[16] Asakura, H.; Teramura, K.; Shishido, T.; Tanaka, T.; Yan, N.; Xiao, C.; Yao, S.; Kou, Y. *In situ* time-resolved DXAFS study of Rh nanoparticle formation mechanism in ethylene glycol at elevated temperature. *Phys. Chem. Chem. Phys.* **2012**, *14*, 2983-2990.
[17] Chu, B.; Liu, T. Characterization of nanoparticles by scattering techniques. *J. Nanopart. Res.* **2000**, *2*, 29-41.
[18] Goyal, P. S.; Aswal, V. K. Use of SANS and SAXS in study of nanoparticles. *Int. J. Nanosci. Ser.* **2005**, *4*, 987-994.
[19] Bentrup, U. Combining *in situ* characterization methods in one set-up: looking with more eyes into the intricate chemistry of the synthesis and working of heterogeneous catalysts. *Chem. Soc. Rev.* **2010**, *39*, 4718-4730.
[20] Sun, Y.; Ren, Y. In Situ Synchrotron X-Ray Techniques for Real-Time Probing of

Colloidal Nanoparticle Synthesis. *Part. Part. Syst. Charact.* **2013**, *30*, 399-419.
[21] Li, T.; Senesi, A. J.; Lee, B. Small Angle X-ray Scattering for Nanoparticle Research. *Chem. Rev.* **2016**, *116*, 11128-11180.
[22] Eisele, F. L.; Hanson, D. R. First Measurement of Prenucleation Molecular Clusters. *J. Phys. Chem. A* **2000**, *104*, 830-836.
[23] Gebauer, D.; Voelkel, A.; Coelfen, H. Stable Prenucleation Calcium Carbonate Clusters. *Science* **2008**, *322*, 1819-1822.
[24] Pouget, E. M.; Bomans, P. H. H.; Goos, J. A. C. M.; Frederik, P. M.; de With, G.; Sommerdijk, N. A. J. M. The Initial Stages of Template-Controlled $CaCO_3$ Formation Revealed by Cryo-TEM. *Science* **2009**, *323*, 1455-1458.
[25] Dey, A.; Bomans, P. H. H.; Muller, F. A.; Frederik, P. M.; de With, G.; Sommerdijk, N. A. J. M.; Will, J. The role of prenucleation clusters in surface-induced calcium phosphate crystallization. *Nat. Mater.* **2010**, *9*, 1010-1014.
[26] Demichelis, R.; Raiteri, P.; Gale, J. D.; Quigley, D.; Gebauer, D. Stable prenucleation mineral clusters are liquid-like ionic polymers. *Nat. Commun.* **2011**, *2*, 590.
[27] Gebauer, D.; kellermeier, M.; Gale, J. D.; Bergström, L.; Cölfen, H. Pre-nucleation clusters as solute precursors in crystallization. *Chem. Soc. Rev.* **2014**, *43*, 2348-2371.
[28] Fermani, S.; Vettraino, C.; Bonacini, I.; Marcaccio, M.; Falini, G.; Gavira, J. A.; Garcia Ruiz, J. M. Heterogeneous crystallization of proteins: Is it a prenucleation clusters mediated process? *Cryst. Growth Des.* **2013**, *13*, 3110-3115.
[29] Hashimoto, T.; Saijo, K.; Harada, M.; Toshima, N. Small-angle x-ray scattering analysis of polymer-protected platinum, rhodium, and platinum/rhodium colloidal dispersions. *J. Chem. Phys.* **1998**, *109*, 5627-5638.
[30] Svergun, D. I.; Shtykova, E. V.; Kozin, M. B.; Volkov, V. V.; Dembo, A. T.; Shtykova, E. V.; Bronstein, L. M.; Platonova, O. A.; Yakunin, A. N.; Valetsky, P. M.; Kholkhlov, A. R. Small-Angle X-ray Scattering Study of Platinum-Containing Hydrogel/Surfactant Complexes. *J. Phys. Chem. B* **2000**, *104*, 5242-5250.
[31] Calandra, P.; Longo, A.; Liveri, V. T. Synthesis of Ultra-small ZnS Nanoparticles by Solid-Solid Reaction in the Confined Space of AOT Reversed Micelles. *J. Phys. Chem. B* **2003**, *107*, 25-30.
[32] Haubold, H.-G.; Vad, T.; Waldöfner, N.; Bönnemann, H. From Pt molecules to nanoparticles: *in-situ* (anomalous) small-angle X-ray scattering studies. *J. Appl. Cryst.* **2003**, *36*, 617-620.
[33] Calandra, P.; Giordano, C.; Longo, A.; Turco Liveri, V. Physiochemical investigation of surfactant-coated gold nanoparticles synthesized in the confined space of dry reversed micelles. *Mater. Chem. Phys.* **2006**, *98*, 494-499.
[34] Tristany, M.; Chaudret, B.; Dieudonné, P.; Guari, Y.; Lecante, P.; Matsura, V.; Moreno-Mañas, Philippot, K.; Pleixats, R. Synthesis of Ruthenium Nanoparticles Stabilized by Heavily Fluorinated Compounds. *Adv. Funct. Mater.* **2006**, *16*, 2008-2015.
[35] Frens, G. Controlled Nucleation for the Regulation of the Particle Size in Monodisperse Gold Suspensions. *Nature-Phys. Sci.* **1973**, *241*, 20-22.
[36] Rusyniak, M.; Abdelsayed, V.; Campbell, J.; El-Shall, M. S. Vapor Phase Homogeneous Nucleation of Higher Alkanes: Dodecane, Hexadecane, and Octadecane. 1. Critical Supersaturation and Nucleation Rate Measurements. *J. Phys. Chem. B* **2011**, *105*, 11866-11872.
[37] Rusyniak, M.; El-Shall, M. S. Vapor Phase Homogeneous Nucleation of Higher Alkanes: Dodecane, Hexadecane, and Octadecane. 2. Corresponding States and Scaling Law Analysis. *J. Phys. Chem. B* **2001**, *105*, 11873-11879.
[38] Abécassis, B.; Testard, F.; Spalla, O.; Barboux, P. Probing in situ the Nucleation and

Growth of Gold Nanoparticles by Small-Angle X-ray Scattering. *Nano Lett.* **2007**, *7*, 1723-1727.
[39] Smith, M. C.; Gilbert, J. A.; Mawdsley, J. R.; Seifert, S.; Myers, D. J. In Situ Small-Angle X-ray Scattering Observation of Pt Catalyst Particle Growth During Potential Cycling. *J. Am. Chem. Soc.* **2008**, *130*, 8112-8113.
[40] Harada, M.; Saijo, K.; Sakamoto, N. Characterization of metal nanoparticles prepared by photoreduction in aqueous solutions of various surfactants using UV-vis, EXAFS, and SAXS. *Colloids Surf. A: Physicochem. Eng. Asp.* **2009**, *349*, 176-186.
[41] Jun, Y.-S.; Lee, B.; Waychunas, G. A. In Situ Observations of Nanoparticle Early Development Kinetics at Mineral—Water Interfaces. *Environ. Sci. Technol.* **2010**, *44*, 8182-8189.
[42] Harada, M.; Tamura, N.; Takenaka, M. Nucleation and Growth of Metal Nanoparticles during Photoreduction Using In Situ Time-Resolved SAXS Analysis. *J. Phys. Chem. C* **2011**, *115*, 14081-14092.
[43] Zheng, N.; Fan, J.; Stucky, G. D. One-Step One-Phase Synthesis of Monodisperse Noble-Metallic Nanoparticles and Their Colloidal Crystals. *J. Am. Chem. Soc.* **2006**, *128*, 6550-6551.
[44] Koerner, H.; MacCuspie, R. I.; Park, K.; Vaia, R. A. In Situ UV/Vis, SAXS, and TEM Study of Single-Phase Gold Nanoparticle Growth. *Chem. Mater.* **2012**, *24*, 981-995.
[45] Wang, J.; Winans, R. E.; Anderson, S. L.; Seifert, S.; Lee, B.; Chupas, P. J.; Ren, Y.; Lee, S.; Liu, Y. In Situ Small-Angle X-ray Scattering from Pd Nanoparticles Formed by Thermal Decomposition of Organo-Pd Catalyst Precursors Dissolved in Hydrocarbons. *J. Phys. Chem. C* **2013**, *117*, 22627-22635.
[46] LaGrow, A. P.; Ingham, B.; Toney, M. F.; Tilley, R. D. Effect of Surfactant Concentration and Aggregation on the Growth Kinetics of Nickel Nanoparticles. *J. Phys. Chem. C* **2013**, *117*, 16709-16718.
[47] St. John, S.; Hu, N.; Schaefer, D. W.; Angelopoulos, A. P. Time-Resolved, in Situ, Small- and Wide-Angle X-ray Scattering To Monitor Pt Nanoparticle Structure Evolution Stabilized by Adsorbed $SnCl_3^-$ Ligands During Synthesis. *J. Phys. Chem. C* **2013**, *117*, 7924-7933.
[48] Wiaderek, K. M.; Borkiewicz, O. J.; Pereira, N.; Ilavsky, J.; Amatucci, G. G.; Chupas, P. J.; Chapman, K. W. Mesoscale Effects in Electrochemical Conversion: Coupling of Chemistry to Atomic- and Nanoscale structure in Iron-Based Electrodes. *J. Am. Chem. Soc.* **2014**, *136*, 6211-6214.
[49] Rose, A. L.; Bilgh, M. W.; Collins, R. N.; Waite, T. D. Resolving Early Stages of Homogeneous Iron(III) Oxyhydroxide Formation from iron(III) Nitrate Solutions at pH 3 Using Time-Resolved SAXS. *Langmuir* **2014**, *30*, 3548-3556.
[50] Chao, Y.; Horner, O.; Vallée, P.; Meneau, F.; Alos-Ramos, O.; Hui, F.; Turmine, M.; Perrot, H.; Lédion, J. In Situ Probing Calcium Carbonate Formation by Combining Fast Controlled Precipitation Method and Small-Angle X-ray Scattering. *Langmuir* **2014**, *30*, 3303-3309.
[51] Schiener, A.; Margerl, A.; Krach, A.; Seifert, S.; Steinrück, H.-G.; Zagorac, j.; Zahn, D.; Weihrich, R. *In situ* investigation of two-step nucleation and growth of CdS nanoparticles from solution. *Nanoscale* **2015**, *7*, 11328-11333.
[52] Mozaffari, S.; Li, W.; Thompson, C.; Ivanov, S.; Seifert, S.; Lee, B.; Kovarik, L.; Karim, A. M. Colloidal nanoparticle size control: experimental and kinetic modeling investigation of the ligand–metal binding role in controlling the nucleation and growth kinetics. *Nanoscale* **2017**, *9*, 13772-13785.
[53] Oestreicher, V.; Huck-Irart, C.; Soler-Illia, G.; Angelomé, P. C.; Jobbágy, M. Mild Homogeneous Synthesis of Gold Nanoparticles through the Epoxide Route: Kinetics,

Mechanisms, and Related One-Pot Composites. *Chem. Eur. J.* **2020**, *26*, 3157-3165.
[54] Castro, N.; Bouet, C.; Ithurria, S.; Lequeux, N.; Constantin, D.; Levitz, P.; Pontoni, D.; Abécassis, B. Insights into the Formation Mechanism of CdSe Nanoplatelets Using in Situ X-ray Scattering. *Nano Lett.* **2019**, *19*, 6466-6474.
[55] Ithurria, S.; Bousquet, G.; Dubertret, B. Continuous Transition from 3D to 1D Confinement Observed during the Formation of CdSe Nanoplatelets. *J. Am. Chem. Soc.* **2011**, *133*, 3070-3077.
[56] Riedinger, A.; Ott, F. D.; Mule, A.; Mazzotti, S.; Knüsel, P. N.; Kress, S. J. P.; Prins, F.; Erwin, S. C.; Norris, D. J. An intrinsic growth instability in isotropic materials leads to quasi-two-dimensional nanoplatelets. *Nat. Mater.* **2017**, *16*, 743-748.
[57] He, H.; Feil, M. W.; Fuchs, S.; Debnath, T.; Richter, A. F.; Tong, Y.; Wu, L.; Wang, Y.; Döblinger, M.; Nickel, B. Growth of Perovskite $CsPbBr_3$ Nanocrystals and Their Formed Superstructures Revealed by In Situ Spectroscopy. *Chem. Mater.* **2020**, *32*, 8877-8884.
[58] Olliges-Stadler, I.; Rossell, M. D.; Süess, M. J.; Ludi, B.; Bunk, O.; Pedersen, J. K.; Birkedal, H.; Niederberger, M. A comprehensive study of the crystallization mechanism involved in the nonaqueous formation of tungstite. *Nanoscale* **2013**, *5*, 8517-8525.
[59] Harada, M.; Asakura, K.; Toshima, N. Structural Analysis of Polymer-Protected Platinum/Rhodium Bimetallic Clusters Using Extended X-ray Absorption Fine Structure Spectroscopy. Importance of Microclusters for the Formation of Bimetallic Clusters. *J. Phys. Chem.* **1994**, *98*, 2653-2662.
[60] Tsai, Y. W.; Tseng, Y. L.; Sarma, L. S.; Liu, D. G.; Lee, J. F.; Hwang, B. J. Genesis of Pt Clusters in Reverse Micelles Investigated by in Situ X-ray Absorption Spectroscopy. *J. Phys. Chem. B* **2004**, *108*, 8148-8152.
[61] Harada, M.; Toshima, N.; Yoshida, K.; Isoda, S. Aggregated structure analysis of polymer-protected platinum/ruthenium colloidal dispersions using EXAFS, HRTEM, and electron diffraction measurements. *J. Colloid Interface Sci.* **2005**, *283*, 64-78.
[62] Harada, M.; Einaga, H. Formation Mechanism of Pt Particles by Photoreduction of Pt Ions in Polymer Solutions. *Langmuir* **2006**, *22*, 2371-2377.
[63] Harada, M.; Einaga, H. In Situ XAFS Studies of Au Particle Formation by Photoreduction in Polymer Solutions. *Langmuir* **2007**, *23*, 6536-6543.
[64] Harada, M.; Inada, Y. In Situ Time-Resolved XAFS Studies of Metal Particle Formation by Photoreduction in Polymer Solutions. *Langmuir* **2009**, *25*, 6049-6061.
[65] Yao, T.; Sun, Z.; Li, Y.; Pan, Z.; Wei, H.; Xie, Y.; Nomura, M.; Niwa, Y.; Yan, W.; Wu, Z.; Jiang, Y.; Liu, Q.; Wei, S. Insights into Initial Kinetic Nucleation of Gold Nanocrystals. *J. Am. Chem. Soc.* **2010**, *132*, 7696-7701.
[66] Ohyama, J.; Teramura, K.; Higuchi, Y.; Shishido, T.; Hitomi, Y.; Kato, K.; Tanida, H.; Uruga, T.; Tanaka, T. In Situ Observation of Nucleation and Growth Process of Gold Nanoparticles by Quick XAFS Spectroscopy. *ChemPhysChem* **2011**, *12*, 127-131.
[67] Ohyama, J.; Teramura, K.; Shishido, T.; Hitomi, Y.; Kato, K.; Tanida, H.; Uruga, T.; Tanaka, T. *In Situ* Au L_3 and L_2 edge XANES spectral analysis during growth of thiol protected gold nanoparticles for the study on particle size dependent electronic properties. *Chem. Phys. Lett.* **2011**, *507*, 105-110.
[68] Ohyama, J.; Teramura, K.; Higuchi, Y.; Shishido, T.; Hitomi, Y.; Aoki, K.; Funabiki, T.; Kodera, M.; Kato, K.; Tanida, H.; Uruga, T.; Tanaka, T. An *in situ* quick XAFS spectroscopy study of the formation mechanism of small gold nanoparticles supported by porphyrin-cored tetradentate passivants. *Phys. Chem. Chem. Phys.* **2011**, *13*, 11128-11135.
[69] Oyanagi, H.; Sun, Z. H.; Jiang, Y.; Uehara, M.; Nakamura, H.; Yamashita, K.; Zhang, L.; Lee, C.; Fukano, A.; Maeda, H. *In situ* XAFS experiments using a microfluidic cell: application to initial growth of CdSe nanocrystals. *J. Synchrotron Rad.* **2011**, *18*, 272-279.

[70] Harada, M.; Kamigaito, Y. Nucleation and Aggregative Growth Process of Platinum Nanoparticles Studied by in Situ Quick XAFS Spectroscopy. *Langmuir* **2012**, *28*, 2415-2428.
[71] Uemura, Y.; Inada, Y.; Niwa, Y.; Kimura, M.; Bando, K. K.; Yagishita, A.; Iwasawa, Y.; Nomura, M. Formation and oxidation mechanisms of Pd–Zn nanoparticles on a ZnO supported Pd catalyst studied by *in situ* time-resolved QXAFS and DXAFS. *Phys. Chem. Chem. Phys.* **2012**, *14*, 2152-2158.
[72] Paclawski, K.; Sikora, M. XAFS in the tracking of reactions in aqueous solution: a case of redox reaction between $[AuCl_4]^-$ complex ions and ethanol. *Arch. Metall. Mater.* **2012**, *57*, 1011-1020.
[73] Yao, S.; Yuan, Y.; Xiao, C.; Li, W.; Kou, Y.; Dyson, P. J.; Yan, N.; Asakura, H.; Teramura, K.; Tanaka, T. Insights into the Formation Mechanism of Rhodium Nanocubes. *J. Phys. Chem. C* **2012**, *116*, 15076-15086.
[74] Tanaka, T.; Ohyama, J.; Teramura, K.; Hitomi, Y. Formation mechanism of metal nanoparticles studied by XAFS spectroscopy and effective synthesis of small metal nanoparticles. *Catal. Today* **2012**, *183*, 108-118.
[75] Ma, J.; Zou, Y.; Jiang, Z.; Huang, W.; Li, J.; Wu, G.; Huang, Y.; Xu, H. An *in situ* XAFS study—the formation mechanism of gold nanoparticles from X-ray-irradiated ionic liquid. *Phys. Chem. Chem. Phys.* **2013**, *15*, 11904-11908.
[76] Gomes, W. C. M.; Neto, A. O. W.; Pimentel, P. M.; Melo, D. M. A.; Silva, F. R. G. An in situ X-ray absorption spectroscopy study of copper nanoparticles in microemulsion. *Colloids Surf. A: Physicochem. Eng. Asp.* **2013**, *426*, 18-25.
[77] Chang, S.-Y.; Gründer, Y.; Booth, S. G.; Molleta, L. B.; Uehara, A.; Mosselmans, J. F. W.; Cibin, G.; Pham, V.-T.; Nataf, L.; Dryfe, R. A. W.; Schroeder, S. L. M. Detection and characterization of sub-critical nuclei during reactive Pd metal nucleation by X-ray absorption spectroscopy. *CrystEngComm* **2016**, *18*, 674-682.
[78] Saeki, M.; Matsumura, D.; Yomogida, T.; Taguchi, T.; Tsuji, T.; Saitoh, H.; Ohba, H. In Situ Time-Resolved XAFS Studies on Laser-Induced Particle Formation of Palladium Metal in an Aqueous/EtOH Solution. *J. Phys. Chem. C* **2019**, *123*, 817-824.
[79] Liu, Y.; Qian, L.; Zhao, X.; Wang, J.; Yao, L.; Xing, X.; Mo, G.; Cai, Q.; Chen, Z.; Wu, Z. Synthesis and formation mechanism of self-assembled 3D flower-like Bi/γ-Fe_2O_3 composite particles. *CrystEngComm* **2019**, *21*, 2799-2808.
[80] Strach, M.; Mantella, V.; Pankhurst, J. R.; Iyengar, P.; Loiudice, A.; Das, S.; Corminboeuf, C.; van Beek, W.; Buonsanti, R. Insights into Reaction Intermediates to Predict Synthetic Pathways for Shape-Controlled Metal Nanocrystals. *J. Am. Chem. Soc.* **2019**, *41*, 16312-16322.
[81] Olliges-Stadler, I.; Stötzel, J.; Koziej, D.; Rossell, M. D.; Grunwaldt, J.-D.; Nachtegaal, M.; Frahm, R.; Niederberger, M. Study of the Chemical Mechanism Involved in the Formation of Tungstite in Benzyl Alcohol by the Advanced QEXAFS Technique. *Chem. Eur. J.* **2012**, *18*, 2305-2312.
[82] Angermund, K.; Bühl, M.; Dinjus, E.; Endruschat, U.; Gassner, F.; Haubold, H.-G.; Hormes, J.; Köhl, G.; Mauschick, F. T.; Modrow, H.; Mörtel, R.; Mynott, R.; Tesche, B.; Vad, T.; Waldöfner, N.; Bönnemann, H. Nanoscopic Pt Colloids in the "Embryonic State". *Angew. Chem. Int., Ed.* **2002**, *41*, 4041-4044.
[83] Angermund, K.; Bühl, M.; Endruschat, U.; Mauschick, F. T.; Mörtel, R.; Mynott, R.; Tesche, B.; Waldöfner, N.; Bönnemann, H.; Köhl, G.; Modrow, H.; Hormes, J.; Dinjus E.; Gassner, F.; Haubold, H.-G.; Vad, T. Kaupp, M. In Situ Study on the Wet Chemical Synthesis of Nanoscopic Pt Colloids by "Reductive Stabilization". *J. Phys. Chem. B* **2003**, *107*, 7507-7515.
[84] Meneau, F.; Sankar, G.; Morgante, N.; Cristol, S.; Catlow, C. R. A.; Thomas, J. M.;

Greaves, G. N. Characterization of zinc oxide nanoparticles encapsulated into zeolite-Y: An in-situ combined X-ray diffraction, XAFS, and SAXS study. *Nucl. Instrum. Meth. B* **2003**, *199*, 499-503.
[85] Benfield, R. E.; Grandjean, D.; Dore, J. C.; Esfahanian, H.; Wu, Z.; Kröll, M.; Geerkens, M.; Schmid, G. Structure of assemblies of metal nanowires in mesoporous alumina membranes studied by EXAFS, XANES, X-ray diffraction and SAXS. *Faraday Discuss.* **2004**, *125*, 327-342.
[86] Beale, A. M.; van der Eerden, A. M. J.; Jacques, S. D. M.; Leynaud, O.; O'Brien, M. G.; Meneau, F.; Nikitenko, S.; Bras, W.; Weckhuysen, B. M. A Combined SAXS/WAXS/XAFS Setup Capable of Observing Concurrent Changes Across the Nano-to-Micrometer Size Range in Inorganic Solid Crystallization Processes. *J. Am. Chem. Soc.* **2006**, *128*, 12386-12387.
[87] Ramallo-López, J. M.; Giovanetti, L.; Craievich, A. F.; Vicentin, F. C.; Marín-Almazo, M.; José-Yacaman, M.; Requejo, F. G. XAFS, SAXS, and HREM characterization of Pd nanoparticles capped with *n*-alkyl thiol molecules. *Physica B* **2007**, *389*, 150-154.
[88] Harada, M.; Kuramitsu, K.; Kimura, Y.; Saijo, K. *In situ* observation of formation of silver particles in water-in-scCO_2 emulsions. *Colloids Surf. A: Physicochem. Eng. Asp.* **2008**, *327*, 21-33.
[89] Abécassis, B.; Testard, F.; Kong, Q.; Francois, B.; Spalla, O. Influence of Monomer Feeding on a Fast Gold Nanoparticles Synthesis: Time-Resolved XANES and SAXS Experiments. *Langmuir* **2010**, *26*, 13847-13854.
[90] Turkevich, J..; Stevenson, P. C.; Hillier, J. A study on the nucleation and growth processes in the synthesis of colloidal gold. *Discuss. Faraday Soc.* **1951**, *11*, 55-75.
[91] Polte, J.; Ahner, T. T.; Delissen, F.; Sokolov, S.; Emmerling, F.; Thünemann, A. F.; Kraehnert, R. Mechanism of Gold Nanoparticle Formation in the Classical Citrate Synthesis Method Derived from Coupled In Situ XANES and SAXS Evaluation. *J. Am. Chem. Soc.* **2010**, *132*, 1296-1301.
[92] Caetano, B. L.; Santilli, C. V.; Meneau, F.; Briois, V.; Pulcinelli, S. H. In Situ and Simultaneous UV—vis/SAXS and UV—vis/XAFS Time-Resolved Monitoring of ZnO Quantum Dots Formation and Growth. *J. Phys. Chem. C* **2011**, *115*, 4404-4412.
[93] Yao, T.; Liu, S.; Sun, Z.; Li, Y.; He, S.; Cheng, H.; Xie, Y.; Liu, Q.; Jiang, Y.; Wu, Z.; Yan, W.; Wei, S. Probing Nucleation Pathways for Morphological Manipulation of Platinum Nanocrystals. *J. Am. Chem. Soc.* **2012**, *134*, 9410-9416.
[94] Xia, F.; Chen, D.; Scarlett, N. V. Y.; Madsen, I. C.; Lau, D.; Leoni, M.; Ilavsky, J.; Brand, H. E. A.; Caruso, R. A. Understanding Solvothermal Crystallization of Mesoporous Anatase Beads by In Situ Synchrotron PXRD and SAXS. *Chem. Mater.* **2014**, *26*, 4563-4571.
[95] Caetano, B. L.; Meneau, F.; Santilli, C. V.; Pulcinelli, S. H.; Magnami, M.; Briois, V. Mechanisms of SnO_2 Nanoparticles Formaiton and Growth in Acid Ethanol Solution Derived from SAXS and Combined Raman–XAS Time-Resolved Studies. *Chem. Mater.* **2014**, *26*, 6777-6785.
[96] Karim, A. M.; Al Hasan, N.; Ivanov, S.; Seifert, S.; Kelly R. T.; Hallfors, N. G.; Benavidez, A.; Kovarik, L.; Jenkins, A.; Winans, R. E.; Datye, A. K. Synthesis of 1nm Pd nanoparticles: Insights on the synthesis mechanism using *in situ* XAFS and SAXS in a microfluidic reactor. *J. Phys. Chem. C* **2015**, *119*, 13257-13267.
[97] Chen, X.; Schröder, J. H.; Hauschild, S.; Rosenfeldt, S.; Dulle, M.; Förster, S. Simultaneous SAXS/WAXS/UV-Vis Study of the Nucleation and Growth of Nanoparticles – A Test of Classical Nucleation Theory. *Langmuir* **2015**, *31*, 11678-11691.
[98] Yang, L.; Cheng, H.; Jiang, Y.; Huang, T.; Bao, J.; Sun, Z.; Jiang, Z.; Ma, J.; Sun F.; Liu, Q.; Yao, T.; Deng, H.; Wang, S.; Zhu, M.; Wei, S. *In situ* studies on controlling an atomically-accurate formation process of gold nanoclusters. *Nanoscale* **2015**, *7*, 14452-14459.

[99] Kabelitz, A.; Guilherme, A.; Joester, M.; Renholz, U.; Radtke, M.; Bienert, R.; Schulz, K.; Schmack, R.; Kraehnert, R.; Emmerling, F. Time-resolved *in situ* studies on the formation mechanism of iron oxide nanoparticles using combined fast-XANES and SAXS. *CrystEngComm* **2015**, *17*, 8463-8470.
[100] Cormary, B.; Li, T.; Liakakos, N.; Peres, L.; Fazzini, P.-F.; Blon, T.; Respaud, M.; Kropf, A. J.; Chaudret, B.; Miller, J. T.; Mader, E. A.; Soulantica, K. Concerted Growth and Ordering of Cobalt Nanorod Arrays as Revealed by Tandem in Situ SAXS-XAS Studies. *J. Am. Chem. Soc.* **2016**, *138*, 8422-8431.
[101] Herbst, M.; Hofmann, E.; Förster, S. Nucleation and Growth Kinetics and ZnO Nanoparticles Studied by in Situ Microfluidic SAXS/WAXS/UV–Vis Experiments. *Langmuir* **2019**, *35*, 11702-11709.
[102] Ramamoorthy, R. K.; Yildirim, E.; Barba, E.; Roblin, P.; Vargas, J. A.; Lacroix, L.-M.; Rodriguez-Ruiz, I.; Decorse, P.; Petkov, V.; Teychené, S.; Viau, G. The role of pre-nucleation clusters in the crystallization of gold nanoparticles. *Nanoscale* **2020**, *12*, 16173-16188.
[103] Christiansen, T .L.; Kjær, E. T. S.; Kovyakh, A.; Röderen, M. L.; Høj, M.; Vosch, T.; Jensen, K. M. Ø. Structure analysis of supported disordered molybdenum oxides using pair distribution function analysis and automated cluster modelling. *J. Appl. Cryst.* **2020**, *53*, 148-158.
[104] Anker, A. S.; Christiansen, T. L.; Weber, M.; Schmiele, M.; Brok, E.; Kjær, E. T. S.; Juhás, P.; Thomas, R.; Mehring, M.; Jensen, K. M. Ø. Structural Changes during the Growth of Atomically Precise Metal Oxido Nanoclsuters from Combined Pair Distribution Function and Small-Angle X-ray Scattering Analysis. *Angew. Chem. Int. Ed.* 10.1002/anie.202103641.